Priscilla Barreto Cardoso

BIOBASED POLYMERIC NANOPARTICLES FROM CASTOR OIL DERIVATIVES BY ADMET AND THIOL-ENE MINIEMULSION POLYMERIZATIONS

Tese submetida ao Programa de Pós-Graduação em Engenharia Química da Universidade Federal de Santa Catarina para a obtenção do Grau de Doutora em Engenharia Química

Orientador: Prof. Dr. Pedro Henrique Hermes de Araújo

Coorientadora: Prof. Dr. Claudia Sayer

Florianópolis
2016

Ficha de identificação da obra elaborada pelo autor
através do Programa de Geração Automática da Biblioteca Universitária da UFSC.

Cardoso, Priscilla Barreto
Biobased polymeric nanoparticles from castor oil derivatives by ADMET and thiol-ene miniemulsion polymerizations / Priscilla Barreto Cardoso ; orientador, Pedro Henrique Hermes de Araújo ; coorientadora, Claudia Sayer. Florianópolis, SC, 2016.
113 p.

Tese (doutorado) - Universidade Federal de Santa Catarina, Centro Tecnológico. Programa de Pós-Graduação em Engenharia Química.

Inclui referências

1. Engenharia Química. 2. Polímeros de fontes renováveis. 3. Polimerização em miniemulsão. 4. Nanopartículas poliméricas. 5. Reações ADMET e tiol-eno. I. Araújo, Pedro Henrique Hermes de. II. Sayer, Claudia. III. Universidade Federal de Santa Catarina. Programa de Pós Graduação em Engenharia Química. IV. Título.

Priscilla Barreto Cardoso

BIOBASED POLYMERIC NANOPARTICLES FROM CASTOR OIL DERIVATIVES BY ADMET AND THIOL-ENE MINIEMULSION POLYMERIZATIONS

Esta Tese foi julgada adequada para obtenção do título de **Doutora em Engenharia Química**, área de concentração de **Desenvolvimento de Processos Químicos e Biotecnológicos**, e aprovada em sua forma final pelo Programa de Pós-Graduação em Engenharia Química da Universidade Federal de Santa Catarina.

Florianópolis, 17 de junho de 2016.

_____
Profª. Drª. Cíntia Soares
Coordenadora do PósENQ

Banca Examinadora:

_____	_____
Prof. Dr. Pedro H. H. de Araújo Orientador	Prof.ª Dr.ª Claudia Sayer Coorientadora
_____	_____
Prof. Dr. Fabrício Machado Silva UnB	Prof. Dr. Reinaldo Giudici USP
_____	_____
Prof. Dr. Marco Di Luccio UFSC	Prof. Dr. Débora de Oliveira UFSC

_____
Prof.ª Dr.ª Cristiane da C. Bresolin
UFSC

ACKNOWLEDGMENTS

Primeiramente, agradeço aos meus orientadores Pedro e Claudia pela oportunidade e pelo privilégio de trabalhar nesse excelente grupo de pesquisa desde a minha iniciação científica (2007). Agradeço de coração por toda motivação, crítica, sugestão, orientação, ombro amigo e pela confiança em mim depositada.

Aos meus pais, Albertina e Edson, e ao meu irmão Murillo, agradeço pelo amor incondicional. Obrigada por sempre terem acreditado em mim e por me incentivarem tanto para que meus planos e sonhos sejam concretizados.

Ao meu namorado Leandro, que surgiu no final desta jornada, mas contribuiu muito para me dar a tranquilidade necessária nesse momento de conclusão. Obrigada por todo o amor, apoio e momentos de descontração. Estás sendo muito importante para mim nesta etapa.

Aos meus amigos e colegas do Laboratório de Controle e Processos de Polimerização (LCP), pela amizade e suporte. Obrigada a todos os que me ajudaram direta ou indiretamente ao longo destes anos colaborando com ideias, discussões sobre resultados ou, até mesmo, com momentos de descontração e desabafo.

I would like to say “Vielen Dank” to Prof. Dr. Michael A. R. Meier, my supervisor during my stay in Germany. Mike, thanks for all the contribution and support, it was a pleasure to work and learn with you. I also want to extend a special "thank you" to my colleagues from the Laboratory of Applied Chemistry (KIT, Germany) for the friendship and all the support which I received, not only with chemistry. It meant a lot and made my time in Germany very pleasant and fun.

Agradeço ao Laboratório Central de Microscopia Eletrônica (LCME/UFSC) pelas imagens de TEM. Ao Laboratório de Propriedades Físicas de Alimentos (PROFI/EQA/UFSC) pelas análises de DSC. Ao Laboratório de Ressonância Magnética Nuclear (LRMN) da UnB, pelas análises de RMN.

Ao Conselho Nacional de Desenvolvimento Científico e Tecnológico (CNPq) e à Coordenação de Aperfeiçoamento de Pessoal de Nível Superior (CAPES) pelo suporte financeiro.

E por último, mas de suma importância, agradeço a Deus pela vida, pela saúde e pela força para realizar e concluir este trabalho. Estou muito satisfeita e feliz ao final desta etapa e só tenho a agradecer por poder concretizar um dos meus maiores sonhos, seguindo esta carreira que tanto almejei desde a minha infância.

Obrigada a todos!

“Green chemistry is replacing our industrial chemistry with nature's recipe book. It's not easy, because life uses only a subset of the elements in the periodic table. And we use all of them, even the toxic ones.”

(Janine Benyus, 1958)

ABSTRACT

Renewable resources are earning special attention as substitutes for petroleum-based compounds, considering the future shortage of fossil supplies and also due to a sense of environmental awareness. In this context, biobased polymers obtained from vegetable oils are considered a promising "green" alternative to fossil-derived polymeric materials and present potential biodegradability and low toxicity, allowing their application for high value added and/or biomedical purposes. Acyclic Diene Metathesis (ADMET) and thiol-ene reactions appear as successful and versatile techniques to obtain high molecular weight polymers from renewable raw materials, enhancing the possibilities for the synthesis of vegetable oil-based polymers via chemical modifications. Additionally, besides avoiding the use of organic solvents, working with an environmentally friendly system, miniemulsion polymerization enables the production of polymeric nanoparticles with unique characteristics and vast commercial interest, with the possibility of using and/or incorporating water-insoluble compounds for a wide range of applications. Herein, it is reported the synthesis and characterization of biobased polymeric nanoparticles using a 100% renewable α,ω-diene-diester monomer obtained by esterification reaction of 10-undecenoic acid (derived from castor oil) with 1,3-propanediol (derived from glycerol, which is also derived from castor oil). ADMET and thiol-ene polymerization reactions were successfully performed in miniemulsion and yielded polymers with weight average molecular weight up to 15 kDa (Mn), depending on different parameters and type of reactants (comonomers, surfactants, catalysts) employed. Then, the poly(thioether-ester) nanoparticles were modified by the oxidation of their sulfur atom to sulfoxide and sulfone groups, aiming the development of nanoparticles with high potential for the encapsulation and release of bioactive compounds. Lastly, results revealed that the synthesized poly(thioether-ester) nanoparticles derived from renewable resources did not present any cytotoxic effect on murine fibroblast (L929) and human cervical cancer (HeLa) cells and showed high blood biocompatibility, assuring their viability for biomedical applications.

Keywords: Biobased polymers. Renewable monomer. ADMET. Thiol-ene reactions. Miniemulsion Polymerization. Polymeric nanoparticles.

RESUMO

Recursos renováveis atraem crescente atenção como substitutos para matérias-primas derivadas do petróleo, considerando a futura escassez de fontes fósseis e também devido a um sentimento de consciência ambiental. Neste contexto, biopolímeros obtidos a partir de óleos vegetais são considerados uma promissora alternativa ecológica aos materiais poliméricos derivados de fontes fósseis, apresentando potencial biodegradabilidade e baixa toxicidade, permitindo sua aplicação para propósitos de alto valor agregado e/ou fins biomédicos. As reações de metátese de dienos acíclicos (ADMET) e tiol-eno aparecem como técnicas bem sucedidas e versáteis para a obtenção de polímeros de elevada massa molar derivados de matérias-primas renováveis, aumentando as possibilidades para a síntese de polímeros derivados de óleos vegetais a partir de modificações químicas. Além disso, a polimerização em miniemulsão é um sistema ambientalmente amigável, livre de solventes orgânicos e permite a produção de nanopartículas poliméricas com características únicas e de grande interesse comercial, com a possibilidade de utilização e/ou incorporação de compostos e compósitos insolúveis em água para uma vasta gama de aplicações, inclusive para fins biomédicos. A possibilidade da obtenção de polímeros em meio aquoso, cuja síntese tradicional é sensível à água, tais como poliésteres, é uma grande vantagem das reações de polimerização ADMET e tiol-eno em miniemulsão. Além disso, muitos outros tipos de materiais podem ser obtidos como, por exemplo, nanocompósitos, nanocápsulas e partículas híbridas. Como vantagem adicional, polímeros que contenham grupos éster na cadeia principal podem sofrer hidrólise, permitindo a sua degradação em ambiente fisiológico, fator de grande importância para aplicações biomédicas ou mesmo para a eliminação do material polimérico no meio ambiente. Dessa forma, o objetivo do presente trabalho foi a síntese e caracterização de nanopartículas poliméricas utilizando um monômero α,ω-dieno-diéster 100% renovável, obtido através da reação de esterificação do ácido 10-undecenoico (derivado do óleo de mamona) com o 1,3-propanodiol (derivado do glicerol, que também é derivado do óleo de mamona). Reações de polimerização ADMET e tiol-eno em miniemulsão foram realizadas com sucesso e produziram polímeros com massa molar média de até 15 kDa (M_n), dependendo de diferentes parâmetros e do tipo de reagentes (comonômeros, surfactantes, catalisadores) utilizados. No estudo das reações ADMET, a grande área superficial da fase orgânica nas reações em miniemulsão provavelmente

aumentou a remoção de etileno (subproduto) do meio reacional, favorecendo a reação ADMET e atingindo polímeros com massas molares maiores do que os polímeros obtidos por polimerização em massa. Através dos resultados obtidos, foi observado que o catalisador Umicore M2 e o surfactante não-iônico Lutensol AT80 formaram a combinação mais adequada para a realização de reações ADMET em miniemulsão. Quando reações tiol-eno foram realizadas em miniemulsão, três diferentes monômeros α,ω-dienos (1,7-octadieno, 1,3-propileno dipenta-1-enoato e 1,3-propileno diundeca-10-enoato) e dois ditióis diferentes (1,4-butanoditiol e 2-mercaptoetil éter) foram testados e os resultados foram comparados. O iniciador AIBN apresentou uma concentração ideal (1 mol%) para a síntese de polímeros com massa molar mais elevada, diferente do comportamento esperado em polimerizações tradicionais via radicais livres. Em seguida, as nanopartículas de poli(tioéter-éster) obtidas foram modificadas através da oxidação do átomo de enxofre em grupos sulfóxido e sulfona, visando à obtenção de nanopartículas com elevado potencial para o encapsulamento e liberação de compostos bioativos. Análises de DLS (Espalhamento Dinâmico de Luz) e MET (Microscopia Eletrônica de Transmissão) asseguraram a estabilidade de tamanho/polidispersão e morfologia das nanopartículas mesmo após o processo de oxidação; análises de FTIR e TGA confirmaram a presença de grupos sulfóxido e sulfona após a oxidação. Por último, foram realizadas análises de biocompatibilidade das nanopartículas de poli(tioéter-éster) obtidas. Resultados revelaram que as nanopartículas de origem renovável não exibiram efeito citotóxico em células de fibroblasto murinho (L929) e câncer cervical humano (HeLa) e, além disso, apresentaram alta hemocompatibilidade, viabilizando futuras aplicações biomédicas como sistemas carreadores de fármacos.

Palavras-chave: Biopolímeros. Monômero renovável. ADMET. Reações tiol-eno. Polimerização em miniemulsão. Nanopartículas poliméricas.

LIST OF FIGURES

LIST OF TABLES

LIST OF ABBREVIATIONS AND ACRONYMS

^{13}C NMR	Carbon Nuclear Magnetic Resonance
^{1}H NMR	Proton Nuclear Magnetic Resonance
AFM	Atomic Force Microscopy
AIBN	Azobisisobutyronitrile
Cat.	Catalyst
$CDCl_3$	Deuterated chloroform
CTAB	Cetyltrimethylammonium Bromide
DLS	Dynamic Light Scattering
DSC	Differential Scanning Calorimetry
DTAB	Dodecyltrimethylammonium Bromide
DTAC	Dodecyltrimethylammonium Chloride
FTIR	Fourier Transform Infrared Spectroscopy
G1	Grubbs 1st Generation
GPC	Gel Permeation Chromatography
HG2	Hoveyda-Grubbs 2nd Generation
Lut80	Lutensol AT 80
PBS	Phosphate Buffered Saline
PDI	Polydispersion Index
PMMA	Poly(methyl methacrylate)
PSD	Particle Size Distribution
SDS	Sodium Dodecyl Sulfate
Surf.	Surfactant
TEM	Transmission Electron Microscopy
THF	Tetrahydrofuran
UM2	Umicore M2

LIST OF SYMBOLS

Dp	Particle Diameter [nm]
M_n	Number Average Molecular Weight [kDa; $kg.mol^{-1}$]
M_w	Weight Average Molecular Weight [kDa; $kg.mol^{-1}$]
nm	Nanometers
ºC	Degree Celsius
T_g	Glass Transition Temperature [ºC]
T_m	Melting Temperature [ºC]
wt.%	Weight-weight Percentage

TABLE OF CONTENTS

CHAPTER I

1 INTRODUCTION

A significant increase of interest in biobased polymers as substitutes for petroleum-based compounds has been observed in the last years, considering the depletion of fossil oil reserves and especially due to a sense of environmental awareness for waste management (MEIER, 2009; TÜRÜNÇ; MEIER, 2011; Z. BEYAZKILIC *et al.*, 2015). In this context, vegetable oils are one of the most important renewable raw materials for the polymer industry due to their relatively low cost, ready availability and value added application possibilities (SHARMA; KUNDU, 2006; BELGACEM; GANDINI, 2008; MEIER, 2011). Moreover, only a few minor modification reactions (if necessary) have to be performed in order to obtain suitable monomers for many different applications (MONTERO DE ESPINOSA; MEIER, 2011).

The main components of vegetable oils are triacylglycerols (triglycerides), which are highly functionalized molecules, and, therefore, have been used in the synthesis of different types of monomers and polymers (GÜNER; YAĞCI; ERCIYES, 2006; MONTERO DE ESPINOSA; MEIER, 2011). Also, the hydrolysis of triglycerides provides glycerol (which is widely used as building block in polymer science finding application in the synthesis of polyurethanes, polyesters, or telomers) and a mixture of saturated and unsaturated fatty acids (that are largely studied as renewable building blocks for the synthesis of polymers with high added value and specific properties). The reactivity of the unsaturated bonds of both triglyceride and isolated fatty acids allows vegetable oils to be employed in a variety of polymerization reactions (KARAK; RANA; CHO, 2009; MUTLU, 2012; TÜRÜNÇ, 2012).

Contributing for sustainable development not only consists in using renewable raw materials, but also involves the application of environmentally friendly and high efficient processes. In this line, metathesis and click chemistry reactions have arisen as a great step forward for "green chemistry" and have opened new paths for the synthesis and modification of polymeric materials with targeted properties (PORRES, 2013; MONTERO DE ESPINOSA; MEIER, 2011). Besides, Acyclic Diene Metathesis (ADMET) and thiol-ene polymerization reactions enhance the possibilities for the synthesis of vegetable oil-based polymers via chemical modifications through the double bonds of α,ω-diene monomers (TÜRÜNÇ; MEIER, 2011).

Organic solvent-free miniemulsion polymerization reactions enable to work with an environmentally friendly system and afford polymeric nanoparticles with microstructures inaccessible by other polymerization techniques (PECHER; MECKING, 2007). In addition, miniemulsion polymerization is a versatile technique and presents some attractive advantages such as easier temperature control and radical compartmentalization inside the polymer particles (promoting high polymerization rates and allowing to obtain high molecular weight polymers) with the possibility of using and/or incorporating water-insoluble compounds for a wide range of applications, including biomedical purposes (EL-AASSER; MILLER, 1997; ASUA, 2002; ANTONIETTI; LANDFESTER, 2002; SCHORK *et al.*, 2005; CARDOSO; ARAUJO; SAYER, 2013).

There is a high demand for polymeric systems that satisfy a number of requirements, such as biodegradability and biocompatibility, for biomedical applications (TÜRÜNÇ; MEIER, 2011). Such novel materials have been widely used in temporary implants, tissue engineering and drug delivery systems (MACHADO; SAYER; ARAÚJO, 2016). In this field, biobased polymers obtained from vegetable oils are considered very promising due to their potential biodegradability (it is possible to include functional groups or even chemical bonds that may facilitate biodegradation) and low toxicity (BIERMANN *et al*., 2000; SHARMA; KUNDU, 2006; LLIGADAS *et al*., 2010).

Based on the above facts, ADMET and thiol-ene polymerization in miniemulsion are being recently investigated (PECHER; MECKING, 2007; 2010; CARDOSO *et al*., 2014; JASINSKI *et al.*, 2014; LOBRY *et al*., 2014; AMATO *et al*., 2015; MACHADO *et al*., 2016), but works portraying the polymerization of renewable monomers through these reactions in aqueous media are still uncommon in the literature (WURM; WEISS, 2014; MACHADO *et al*., 2016). Furthermore, apart from the advantages already mentioned, ADMET and thiol-ene reactions allow the synthesis of high molecular weight polyesters in aqueous dispersed medium and thereby are suitable for the production of polymeric nanoparticles containing ester groups in the main chain, which can undergo hydrolysis (RYDHOLM; BOWMAN; ANSETH, 2005; RYDHOLM; ANSETH; BOWMAN, 2007) enabling their degradation in physiological environment. These characteristics are of great importance for biomedical applications or material disposal (JASINSKI *et al.*, 2014; MACHADO; SAYER; ARAÚJO, 2016).

1.1 OBJECTIVES

1.1.1 General Objectives

This work, in collaboration with Professor Dr. Michael A. R. Meier from the Karlsruhe Institute of Technology (KIT) - Germany, aims to investigate the synthesis of a castor oil-derived monomer and its subsequently use in ADMET (Acyclic Diene Metathesis) and thiol-ene polymerization reactions in miniemulsion, in order to obtain biobased polymeric nanoparticles and also compare the results with the polymerization in bulk.

1.1.2 Specific Objectives

- Synthesis and characterization of a fully renewable α,ω-diene diester monomer using castor oil derivatives as chemical platforms.

ADMET reaction

- Synthesis and characterization of polymeric nanoparticles through ADMET reactions in miniemulsion using the synthesized α,ω-diene diester monomer; bulk reactions for comparison;
- Evaluation of the influence of temperature and type of surfactant and catalyst in ADMET reactions in miniemulsion.

Thiol-ene polymerization

- Synthesis and characterization of polymeric nanoparticles through thiol-ene polymerization in miniemulsion using the synthesized α,ω-diene diester monomer; bulk reactions for comparison;
- Evaluation of the influence of type of diene and dithiol monomers, initiator concentration and type of surfactant on the polymer molecular weight;
- Oxidation of the obtained poly(thioether-ester) nanoparticles to poly(sulfone-ester), aiming different thermal properties;
- Characterization of the obtained oxidized polymers regarding structure, thermal properties and morphology.

CHAPTER II

2 REVIEW

This Chapter presents a brief review about the subjects discussed in this thesis. Firstly, the synthesis of vegetable oils-derived monomers for the production of new polymers is introduced. Then, metathesis and thiol-ene reactions are presented, describing characteristics, conditions and applications. Lastly, miniemulsion polymerization is discussed, with its mechanisms and specificities.

2.1 SYNTHESIS OF MONOMERS FROM VEGETABLE OILS

Currently, vegetable oils are one of the most important sources of renewable raw materials for the chemical industry (in Germany, for example, 30% of the 2.7 million tons of raw materials from renewable sources consumed in 2005 were vegetable oils) and they are widely used for manufacturing surfactants, cosmetics and lubricants (MEIER; METZGER; SCHUBERT, 2007). These renewable raw materials show great potential as sustainable resources for the polymer industry because the synthetic potential of naturally occurring fatty acids can be exploited for monomer and polymer synthesis without many reaction steps. Additionally, thermoplastic materials having linear and hyperbranched architectures, resulting in polymers with tunable properties, can be prepared from fatty acids and their derivatives (TÜRÜNÇ, 2012; KARAK; RANA; CHO, 2009).

According to Meier (2011), the use of vegetable oils as a renewable raw material in the polymer industry is a challenge and an opportunity that may allow the replacement of existing polymerization processes based on petroleum compounds. This approach is not only environmentally friendly (green chemistry) because the potential use of renewable natural resources is exploited in an efficient manner, but it will also be necessary in a few decades due to the depletion of fossil resources.

The main constituents of vegetable oils are triacylglycerols (Figure 1), derived from the esterification of glycerol with three fatty acids, which make up 95% of the total weight of triglycerides. Depending on the fatty acids content, each vegetable oil has specific chemical and physical properties (MONTERO DE ESPINOSA; MEIER, 2011; GÜNER; YAĞCI; ERCIYES, 2006), which are affected by the stereochemistry of the double bonds of the fatty acids chains, the

unsaturation degree and the carbon chain length (MEIER, METZGER; SCHUBERT, 2007).

Figure 1. Chemical structure of triglycerides. R_1, R_2 e R_3 correspond to the fatty acid chains.

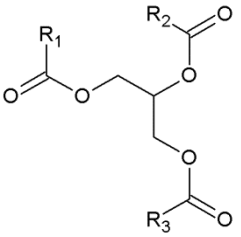

Source: Author.

Depending on the used vegetable oils, the separation process can lead to a wide variety of fatty acids (saturated or unsaturated), each one having different types of functional groups (-OH, epoxy, triple bonds, etc.). Table 1 presents the fatty acid content and number of double bonds per triglyceride of the most common commodity vegetable oils.

Table 1. Fatty acids composition of the most common vegetable oils.

Vegetable Oil	Fatty Acids Content (%)					(DB/TG)[a]
	Palmitic	Stearic	Oleic	Linoleic	Linolenic	
Castor[b]	0.9	0.8	2.9	4.5	0.6	-
Corn	10.9	2.0	25.4	59.6	1.2	4.5
Linseed	5.5	3.5	19.1	15.3	56.6	6.6
Palm	44.4	4.1	39.3	10.0	0.4	1.8
Soybean	11.0	4.0	23.4	53.2	7.8	4.6

[a] double bond per triglyceride.
[b] castor oil contains 87.7 – 90.4 % of ricinoleic acid.

Source: LU; LAROCK, 2009.

Due to the different functional groups of the fatty acids, these renewable raw materials can be used for the synthesis of new monomers that may be used in catalytic metathesis reactions, free radical polymerization, controlled/living polymerization as well as polycondensation reactions through functional groups present in the molecule, yielding polyesters, polyamides, polyethers and

functionalized polyolefins (MEIER, 2009). The most commonly fatty acids used in polymer chemistry are: oleic, linoleic, linolenic, ricinoleic and erucic acids; their structures are shown in Figure 2.

Figure 2. Chemical structures of the fatty acids most commonly used in the polymer chemistry. (a) oleic, (b) linoleic, (c) linolenic, (d) ricinoleic, (e) erucic.

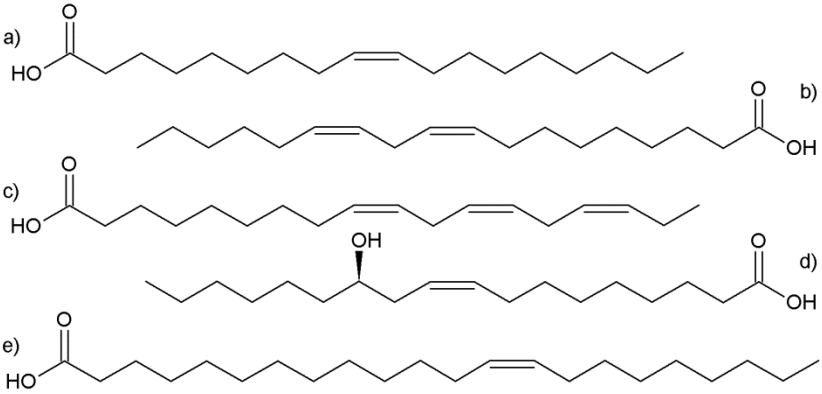

Source: Adapted from ESPINOSA; MEIER, 2011.

Typically, a triglyceride chain presents 5 chemically reactive sites, shown in Figure 3, suitable for posterior modification and synthesis of different types of monomer (MUTLU, 2012). However, researches about chemical modifications of vegetable oils basically present simple variations of the acyl group of the fatty acid. Regarding the use of vegetable oils and fatty acids in chemical industries, the most classic and well-established chemical transformations is directed to the carboxyl and ester groups and relatively underachieved in the side chain (MEIER; METZGER; SCHUBERT, 2007; GANDINI, 2008; RONDA *et al.*, 2011; MONTERO DE ESPINOSA; MEIER, 2011). When using these conventional modification reactions in the carboxylic group, fatty acids are converted into fatty alcohols, soaps, esters, thioesters, amides or amines hydrazides (KREUTZER, 1984; HEDMAN *et al.*, 2003; TAKAGAKI *et al.*, 2006; BARRAULT; POUILLOUX, 1997).

In the past few decades, the selective functionalization of the fatty acids alkyl chains has been extensively researched with particular attention to the double bond of unsaturated compounds. Surprisingly, only a few reactions using the double bond of unsaturated fatty compounds are currently applied in the chemical industry:

hydrogenation, epoxidation and ozone cleavage (BIERMANN *et al.*, 2011). Radical, electrophilic, nucleophilic and also pericyclic additions to the double bond of unsaturated fatty acids may lead to a large number of novel oleochemicals with interesting characteristics.

Figure 3. Reactive sites of a generic triglyceride.

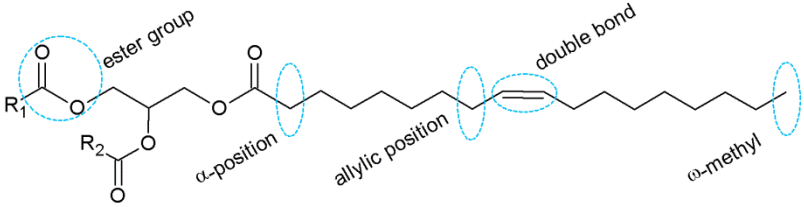

Source: Adapted from MUTLU (2012).

Regarding chemical modifications through the double bonds, olefin metathesis and thiol-ene reactions appear as alternative and efficient processes, enhancing the possibilities for synthesis of vegetable oil-based polymers. These two types of reactions are described separately in the following sections (2.2 e 2.3).

2.1.1 Castor oil as renewable raw material

In addition to the above mentioned possible chemical modifications of existing reactive sites in triglycerides, some fatty acids naturally present different functional groups in their alkyl chains. Today, the only commercial source of a substituted fatty acid is castor oil, cultivated all over the world in temperate zones (MUTLU, 2012). Castor oil is a triglyceride composed of fatty acids and glycerol, like any other vegetable oil, and 90% of its fatty acid content consists of ricinoleic acid - whose carbon chain has a hydroxyl, a very reactive radical. The high level of this fatty acid is the reason for the high value of castor oil and its several application possibilities in the chemical industry (MUTLU; MEIER, 2010).

Pyrolysis of castor oil (Figure 4) splits the ricinoleate molecule in heptaldehyde and undecenoic acid, as well as light gases and a small fraction of free fatty acids (saturated and unsaturated) from C10 to C18. These two products, heptaldehyde and 10-undecenoic acid, are important raw materials for cosmetics (C11 and C7 aldehydes are used in soaps, shampoos, talcum powders and perfume formulations),

pharmaceutical and polymeric compounds. Furthermore, heptaldehyde is used as a solvent for rubbers, resins and plastics and 10-undecenoic acid may be directly used for applications as bactericides and fungicides agents (MUTLU; MEIER, 2010).

Additionally, 10-undecenoic acid proved to be an important precursor for the synthesis of antitumor compounds, antibiotics and, especially, is one of the oldest renewable "building blocks" used in the industry as precursor for Nylon 11 (MUTLU; MEIER, 2010; VAN DER STEEN; STEVENS, 2009). Due to the presence of hydroxyl groups in its chain, castor oil can be used in the synthesis of a wide variety of polyurethane products, ranging from coatings, thermoplastic elastomers, rigid and semi-rigid foams, sealants and adhesives for flexible foams, clearly showing that castor oil is one of the most promising renewable raw materials for the chemical and polymer industry (SHARMA; KUNDU, 2008; PETROVIC, 2008; MUTLU, 2012).

Figure 4. Synthesis of two of the most used chemicals in the chemical industry, derived from castor oil by pyrolysis: heptaldehyde and 10-undecenoic acid.

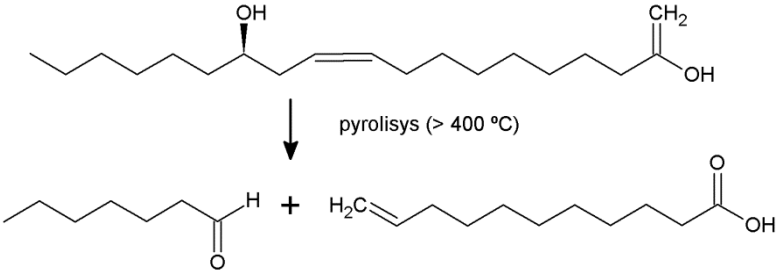

Source: Author.

2.2 OLEFIN METATHESIS

Among the wide range of organic and organometallic reactions allowing obtaining new unsaturated molecules, olefin metathesis appears as a very versatile tool that enables chemical transformations that were challenging (or even impossible) to perform by any other means (RYBAK; FOKOU; MEIER, 2008). Through metathesis reactions it is possible to obtain structurally simple olefins having different chain lengths and unsaturation degrees, as well as mono- and diesters compounds (IVIN; MOL, 1997).

Olefin metathesis, or transalkylidenation, is a chemical reaction involving the position (in Greek: *tithemi*) exchange (*meta*) of alkene

fragments generated by the scission of carbon-carbon double bonds. The term "olefin metathesis" was firstly introduced by Calderon and coworkers in 1960, although there were already reports of transalkilidenation reactions since 1950 (CALDERON; CHEN; SCOTT, 1967; CALDERON, 1972). Proposed for the first time by Hérisson and Chauvin in 1971, the accepted mechanism for this transformation reaction proceeds, in a reversible manner, through a cycloaddition [2 + 2] of an olefinic double bond with a metallocarbene, and the consequent cycloreversion of the metallacyclobutane in the opposite sense leads to a new olefin and a metal alkylidene, as shown in Figure 5 (HÉRISSON; CHAUVIN, 1971).

Figure 5. Mechanism for the olefin metathesis reaction proposed by Chauvin.

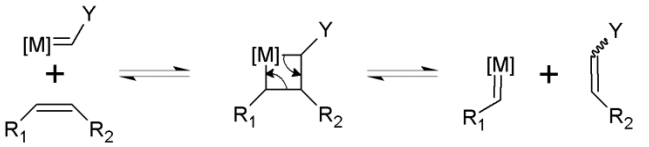

Source: Adapted from HÉRISSON; CHAUVIN (1971).

Olefin metathesis, as depicted in Figure 6, occurs mostly via five kinds of chemical reactions, including ring-opening metathesis (ROM), ring-closing metathesis (RCM), ring-opening metathesis polymerization (ROMP), acyclic diene metathesis polymerization (ADMET) and cross-metathesis (CM) (MUTLU, 2012; MATOS *et al.*, 2007). Cross-metathesis is a reaction using olefins from two different types, ring-opening metathesis is characterized by the formation of non-conjugated dienes from cyclic olefins and it is the reverse reaction of the ring-closing metathesis. In addition, polymerization reactions may occur between acyclic dienes (ADMET) or involving a chain-growth of cyclic alkenes to linear unsaturated polymers (ROMP) (FREDERICO; BROCKSOM; BROCKSOM, 2005).

Metathesis reactions are generally reversible and, with an appropriate catalyst system, equilibrium can be reached in a matter of seconds, even with substrate/catalyst ratios of 10^4 (IVIN; MOL, 1997). Despite being an excellent tool for organic synthesis, studies about olefin metathesis reaction had only a significant advance since the 90s, after the development of organometallic compounds by Schrock and Grubbs (IVIN; MOL, 1997). The Schrock catalysts, based on neutral tungsten and molybdenum alkylidene complexes, are highly reactive

towards different substrates with different steric and electronic variations, capable of reacting with internal and terminal olefins, but they show sensitivity to polar functional groups, humidity, oxygen, and impurities present in the solvent, restricting their usage (SCHROCK *et al.*, 1980).

Figure 6. Most important types of olefin metathesis reactions: CM (Cross-Metathesis), RCM (Ring Closing Metathesis), ROM (Ring Opening Metathesis), ROMP (Ring Opening Metathesis Polymerization) and ADMET (Acyclic Diene METathesis).

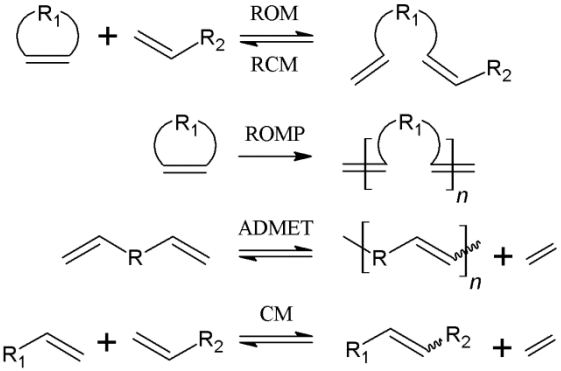

Source: Author.

Kinetic and mechanistic studies were fundamental to the development of the so-called well-defined catalysts for metathesis reactions, known as first and second-generation Grubbs catalysts, which are ruthenium catalytic systems, more robust in air and with various polar functional groups. Furthermore, these catalysts enable reactions under mild conditions, such as atmospheric pressure and temperatures below 100 °C, which may be conducted in common solvents without prior purification (GRUBBS, 2004). In 2005, Robert H. Grubbs, Yves Chauvin and Richard R. Schrock shared the Noble Prize in chemistry for their contributions to olefin metathesis (MATOS *et al.*, 2007; FERREIRA; SILVA, 2005).

2.2.1 ADMET polymerization

The development of Acyclic Diene Metathesis (ADMET) polymerizations, as for all metathesis reactions, has been closely linked

to the development of catalysts presenting improved activity, selectivity and stability (MUTLU; MONTERO DE ESPINOSA; MEIER, 2011).

The ADMET reaction has been intensively studied since Wagener and colleagues (1990a; 1990b) reported the first examples of high molecular weight polymers obtained by polymerization of α,ω-dienes. This reaction follows a step-growth mechanism and it is driven by the release of a low molecular weight condensate, usually ethylene (Figure 7). This metathesis reaction produces well-defined and strictly linear polymers with (modified) unsaturated polyethylene backbones (BAUGHMAN; WAGENER, 2005) and can only reach high molecular weights at high monomer conversion, like all traditional condensation polymerizations (MUTLU; MONTERO DE ESPINOSA; MEIER, 2011).

Figure 7. Schematic representation of an ADMET (Acyclic Diene METathesis) polymerization.

Source: Adapted from MUTLU; MONTERO DE ESPINOSA; MEIER (2011).

The mechanism of the ADMET polymerization cycle is well established (Figure 8). The olefin coordinates to a metal-carbene complex, and then a cycloaddition reaction occurs forming a metallacyclobutane intermediate (1). At this stage, the productive cleavage of the intermediate complex (1) leads to the formation of the alkylidene complex (2). A subsequent reaction with the double bond of another diene produces a metallacyclobutane ring (3), which subsequently leads to the polymer formation. The cycle continues with the coordination of another diene or growing polymer, followed by productive cleavage and release of ethylene. Once all the species involved in the catalytic cycle are in equilibrium, ethylene is generally removed from the reaction medium by applying vacuum or using a constant flow of an inert gas, such as argon or nitrogen, promoting the polymer formation (MUTLU, 2012).

The discovery and usage of the Schrock and Grubbs catalysts paved the way for the synthesis of polymers with different architectures and functionalities through ADMET reactions. For example, applications of the ADMET reaction enabled the development of synthetic routes for obtaining perfectly linear polyethylenes and a wide range of polyethylenes functionalized and branched with alkyl groups

specifically placed along their main chain (OPPER; WAGENER, 2011). Graft copolymers with “perfect comb” structures are also accessible via polymerizing ADMET (O’DONNELL *et al*., 2001).

Figure 8. ADMET polymerization mechanism.

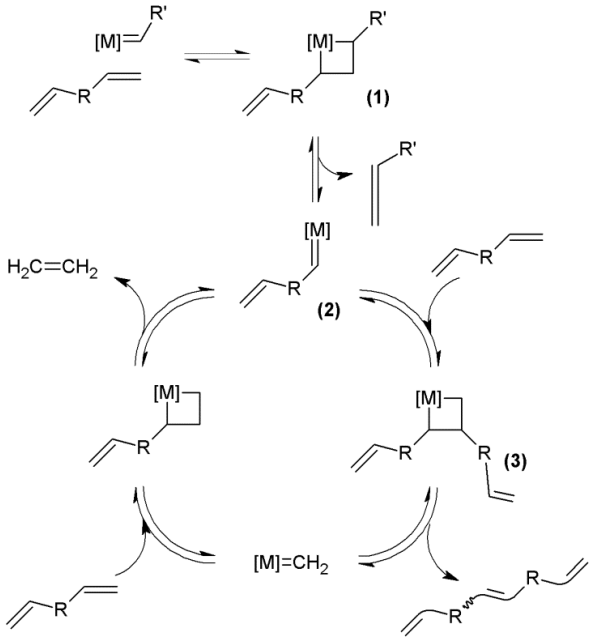

Source: Adapted from MUTLU; MONTERO DE ESPINOSA; MEIER (2011).

Recently, Meier and coworkers (RYBAK; MEIER, 2008; MONTERO DE ESPINOSA *et al*., 2009; MUTLU *et al.*, 2010; FOKOU; MEIER, 2010) investigated the synthesis and posterior polymerization of α,ω-diene monomers derived from vegetable oils. Using 10-undecenoic acid (which is the major product of castor oil pyrolysis) due to its terminal olefin, different types of α,ω-dienes were prepared and submitted to ADMET reactions for obtaining new polymeric structures. Thus, acyclic diene metathesis (ADMET) reaction is a promising technique to obtain high molecular weight polymers from renewable raw materials (WARWEL *et al.*, 2001; MEIER; METZGER; SCHUBERT, 2007).

2.3 THIOL-ENE REACTIONS

The first publication on addition of mercaptans to unsaturated compounds was in 1905 when Posner noted that thiols and alkenes could react spontaneously with each other or in the presence of an acid (POSNER, 1905). In 1926, thiol-ene reactions were presented as a polymerization reaction for the very first time, when Braun and Murjahn found out that alkyl mercaptans spontaneously gelled upon heating (BRAUN; MURJAHN, 1926). However, the widespread polymerization mechanism mediated by free radicals, including the individual steps of the reaction, was only elucidated by Kharasch, Read and Mayo (1938) just before the Second World War in 1938 (CLAUDINO, 2011).

In the half of the twentieth century, thiol-ene chemistry was a widely used method for crosslinking polymers, but the technique fell out of favor due to the preference for high molecular weight polymers which were not covalently cross-linked (KADE; BURKE; HAWKER, 2010). Currently, thiol-ene chemistry is especially used for the biofunctionalization of polymers and particles/nanoparticles surfaces for biomedical usages; however, there are several different applications such as UV curable resins, high impact absorption materials, electronic coating and others (STENZEL, 2013; HOYLE; LEE; ROPER, 2004).

Thiol-ene reactions are based on easily abstractable hydrogens of the thiol group due to the low energy of the sulfur-hydrogen bond ($RS^{\delta}—H^{\delta+}$), 368.44 $kJ.mol^{-1}$. It occurs because the electron-poor hydrogen atom is bonded to a sulfur atom, which is not as electronegative as an oxygen atom of an alcohol group (for example, the energy of the OH bond of a methyl alcohol (MeO—H) is 435.43 $kJ.mol^{-1}$). Disruption of the S-H bond may occur through direct photolysis or thermolysis, or indirectly via nucleophilic initiators which generate free radicals and chemically attack the thiol group; this bond cleavage generates electrophilic thiyl radicals (RS•) which are extremely reactive and can be added to a wide diversity of unsaturated compounds. The addition reaction, known as hydrothiolation of C=C bonds, is exothermic, typically between -10.5 and -22.6 $kcal.mol^{-1}$, and energetically favorable because a carbon-carbon σ-bond (~370 $kJ.mol^{-1}$) is formed instead of a π-bond, weaker (~235 $kJ.mol^{-1}$) (HOYLE; BOWMAN, 2010).

2.3.1 Thiol-ene polymerization

Like a traditional free-radical polymerization, thiol-ene polymerization reaction proceeds divided into three stages: initiation, propagation and termination, plus a chain transfer step (Scheme 1). Firstly occurs a thermal decomposition of the initiator in a pair of active radicals and the reaction of a thiol with an active radical produced, resulting in a primary radical RS● (I). Propagation involves a reaction between RS● and an alkene, generating an intermediary compound (II); thus, the intermediary compound abstracts a hydrogen from another molecule of thiol (III), resulting in the thiol-ene addition product and a new radical RS●. Termination (IV, V, VI) occurs through radical (RS● or carbon-centered radical) combination rather than dispropornation (CARLSON; KNIGHT, 1973).

Scheme 1. Thiol-ene reaction steps: initiation (I), propagation (II), chain-transfer step (III) and termination (IV, V and VI).

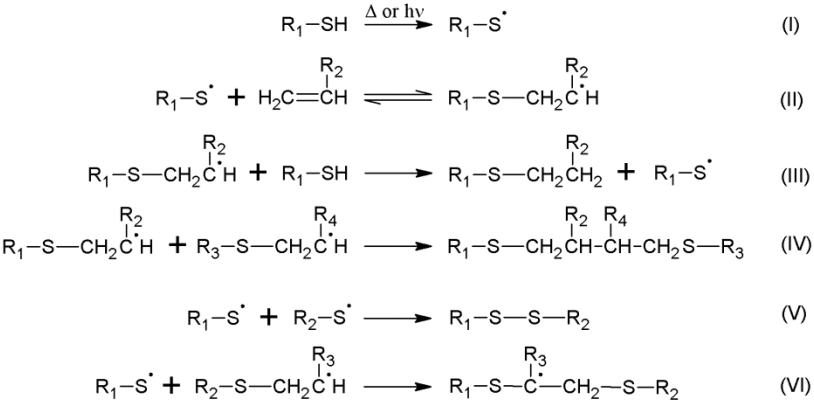

Source: Author.

Figure 9 presents the characteristic two steps mechanism of the thiol-ene polymerization reaction, divided into initiation, propagation and termination, as mentioned above. Firstly, the reaction begins with the thiol decomposition into thiyl radicals through hydrogen abstraction, which can be induced by photo- or thermoinitiation with the aid or not of initiators. The resulting thiyl radical is then added to one of the double bonds of the diene (step I), generating an intermediary β-carbon radical, followed by the chain transfer to a second thiol (step II),

resulting in the primary product of the thiol-ene addition, which still possess a double bond available for the propagation of the polymer chain. Once the mechanism regenerates the thiyl radical, there is no consumption of the thiol groups and, hence, the polymerization continues in a cyclic sequence. Termination reactions are often considered insignificant compared to the propagation rates and generally involve bimolecular combination of β-carbon or thiyl radicals, although these processes have not yet been fully elucidated (CLAUDINO, 2011).

Figure 9. Propagation cycle of a thiol-ene polymerization: addition of a thiyl radical to a double bond (I); chain-transfer from a carbon-centered radical to a thiol-group.

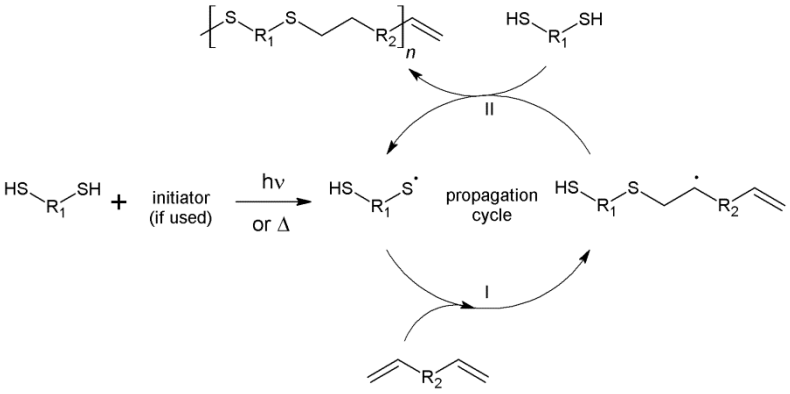

Source: Adapted from CLAUDINO (2011).

Thiol-ene addition kinetics is strongly influenced by the type of the unsaturated compound (terminal, internal, conjugated, non-conjugated and substituted) and, depending on the thiol structure, the reactivity order can be slightly modified (HOYLE; BOWMAN, 2010; LOWE, 2010). Hoyle, Lee and Roper (2004) classified the reactivity of certain unsaturated compounds in thiol-ene addition as follows: Norbornene > Vinyl ether > Propenyl > Alkene ~ Vinyl ester> N-Vinyl amides > Allyl ether ~ Allyltriazine ~ Allylisocyanurate > Acrylate > Unsaturated ester > N-substituted maleimide > Acrylonitrile ~ methacrylate > Styrene > Conjugated dienes. Additionally, it was found that 1-hexene is 8 times more reactive than trans-2-hexene and 18 times more reactive than trans-3-hexene, showing the strong effect of the double bond position in the alkene compound.

One of the most important advantages offered by the thiol-ene chemistry over classical free-radical polymerizations is the high ability to overcome oxygen inhibition. In the case of radical polymerization using (meth)acrylates, the oxygen interacts with the radical of a growing polymer chain and the chain will immediately terminate due to the formation of an alkyl peroxy radical, which has insufficient reactivity to continue the propagation step, resulting in short chains fragments (HOYLE *et al*., 2003). In turn, for thiol-ene polymerization reactions, the formation of such radicals due to oxygen presence does not inhibit the polymerization because peroxy radicals are capable of abstracting the hydrogen from thiol groups and thus generate thiyl radicals, continuing the propagation step with new alkenes. Therefore, the presence of oxygen in thiol-ene reactions has only a minimal effect on the main reaction route but does not affect their products (O'BRIEN; CRAMER; BOWMAN, 2006). As hydrogen donor groups, thiols can be added (even in small amounts) to formulations with acrylic monomers to suppress oxygen inhibition in the polymerization reaction, by trapping the peroxy radicals.

Although known for over a century, thiol-ene addition reactions have become very popular in the recent years due to their "click" characteristics, such as speed, robustness and efficiency, as well as low formation of by-products (HOYLE; BOWMAN, 2010). Even though the efficiency of this type of reaction requires terminal unsaturation and strongly depends on the thiol used, polymerization reactions of α,ω-dienes with dithiols have been successfully applied in order to obtain a wide variety of new polymers (KREYE; TOTH; MEIER, 2011; TÜRÜNÇ; MEIER, 2012; 2013; FIRDAUS *et al.*, 2014).

For being an effective tool in several areas, used for polymerization, curing and polymer modification reactions, thiol-ene reactions may be considered as a versatile and efficient tool for the synthesis of monomers and high added-value chemicals, and also for synthesis and modification of polymers derived from fully renewable α,ω-diene monomers bearing, for example ester, ether, or amide functional groups in the backbone chain (MACHADO; SAYER; ARAÚJO, 2016). In addition, by using monomers with different functionalities, it is possible to tune some properties of the monomer, such as degradability, crosslinking, shrinkage stress and other physical features.

Due to their electronically rich double bonds, vegetable oils and derivatives allow the radical addition of different types of molecules, especially thiols (MUTLU, 2012). Examples of reactions between

vegetable oils or derivatives and thiols are found in the literature, such as the synthesis of telechelic alcohols from 10-undecenoate allyl by thiol-ene addition with mercaptoethanol (LLUCH *et al.*, 2010); the functionalization of methyl 10-undecenoate, a derivative of castor oil, with mercaptoethanol or 1-thioglycerol (TÜRÜNÇ; MEIER, 2010); the copolymerization of fatty acid derivatives with ferulic acid derived compounds with 1,4-butanedithiol (KREYE; TOTH; MEYER, 2011), and others.

Apart from the already mentioned advantages, thiol-ene reactions are considered environmentally friendly because may be carried out without solvent, under mild reaction conditions (by photochemical initiation, for example) and without using catalysts consisting of potentially toxic metal compounds, commonly employed in other "click" reactions (KADE; BURKE; HAWKER, 2010; HOYLE; LOWE; BOWMAN, 2010). In addition, biocompatible and biodegradable polymers can be synthesized through thiol-ene polymerization for biomedical application (WANG *et al*., 2013; VANDENBERGH *et al*., 2014; AMATO *et al*., 2015).

2.4 MINIEMULSION POLYMERIZATION

Over the last years, miniemulsion polymerization has been earning importance and the development of innovative and more accessible polymeric materials obtained by this technique has become more common due to the combination of some attractive advantages such as the absence of solvents, easier temperature control, and radical compartmentalization inside the polymer particles (promoting high polymerization rates and allowing to obtain high molecular weight polymers) with the possibility of using and/or incorporating water-insoluble reactants and compounds (EL-AASSER; MILLER, 1997; ASUA, 2002; ANTONIETTI; LANDFESTER, 2002; SCHORK *et al.*, 2005), such as several vegetable oils (CARDOSO; ARAUJO; SAYER, 2013).

Miniemulsions are characterized by a heterophase system in which submicrometric droplets (size ranging from 50 to 500 nm) of the monomer phase (which are formed with the aid of high shear devices) are dispersed in a continuous phase, usually water. In these systems, the small droplets are protected against coalescence by using an appropriate surfactant and the monomer diffusion can be controlled by the addition of a costabilizer (LANDFESTER *et al.*, 1999; ASUA, 2002;

LANDFESTER, 2006). A simplified schematic of the miniemulsion polymerization process is shown in Figure 10.

Figure 10. Principle of miniemulsion polymerization.

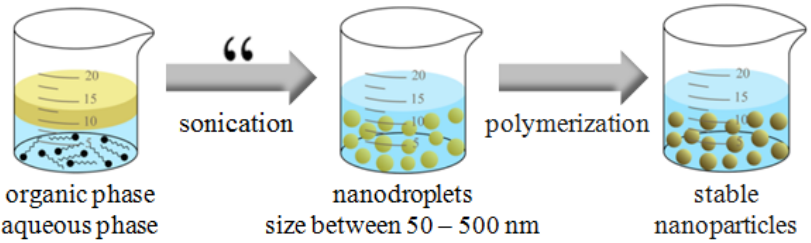

Source: Adapted from Landfester (2006).

In contrast to emulsion polymerization, that presents micellar nucleation, miniemulsion polymerization features droplet nucleation and, therefore, each droplet is the polymerization *locus*, acting like a bulk polymerization nanoreactor (UGELSTAD; EL-AASSER; VANDERHOFF, 1973). According to Asua (2002), not every droplet is necessarily nucleated. Nevertheless, the fact that all or nearly all droplets are nucleated allows the reduction or total elimination of the need for mass transport of the monomer in the aqueous phase, featuring an important advantage of the miniemulsion polymerization process compared to conventional emulsion.

In addition to the droplets nucleation, other nucleation mechanisms may possibly occur, such as micellar and homogeneous nucleation. Therefore, miniemulsion systems require an evaluation of the necessary parameters for the maximization of droplet nucleation. As mentioned by Asua (2002), if water-soluble initiators are used, the droplets nucleation depends on a sequence of processes. First, there is radical formation in the aqueous phase by the initiator decomposition. Due to the high water solubility of the radicals, they are not able to enter the monomer droplets or micelles. Thus, the radical polymerization starts in the aqueous phase by monomer desorption from the droplets, resulting in oligomers. As the oligomers grow, they become more hydrophobic until they reach a critical length and then enter the monomer droplets, characterizing the droplets nucleation, or even enter the pre-existing micelles, the so-called micellar nucleation. If the radical grows until it reaches a second critical size, further increasing its hydrophobicity and inhibiting its entry in the nanodroplets, this growing

oligomer precipitates, yielding a new particle and featuring a homogeneous nucleation (GILBERT, 1995).

It is known that the surfactant concentration in miniemulsions should be below the critical micelle concentration (CMC) in order to prevent the formation of micelles. In the absence of micelles, the droplets nucleation depends only on the number of radicals which enters the nanodroplets, whilst the resultant radicals precipitate in the aqueous phase (homogeneous nucleation). However, Hansen and Ugelstad (1979) observed that the presence of micelles also depends on the homogenization process used. Using hexadecane as costabilizer and applying a low-intensity agitation, the authors reported the formation of large droplets of monomer, decreasing the total surface area of nanodroplets and, consequently, causing the presence of free surfactant in the aqueous phase, yielding micelles and favoring micellar nucleation. In contrast, increasing the dispersion intensity resulted in smaller droplets and the absence of micelles. Therefore, it can be concluded that micelles formation should be avoided combining proper homogenization conditions and surfactant concentration below the CMC in the aqueous phase.

The nucleation mechanisms discussed to this point refer to polymerization in miniemulsion carried out with a water soluble initiator, because when an organic-soluble initiator is applied, the nucleation of the monomer droplets is predominant, since the initiator is already inside the drop. For this reason, organic-soluble initiators can reduce homogeneous nucleation and diffusional degradation occurrences, once the radicals are generated inside the droplets and there is no need for mass transfer of the monomer through the aqueous phase. However, the small volume of the nanodroplets limits the efficiency of the hydrophobic initiator due to the higher probability of recombination of the newly formed radicals (AUTRAN; CAL; ASUA, 2007).

Once the miniemulsions are formed, there are two mechanisms (shown in Figure 11) which can change the number and size of the droplets: diffusional degradation (Ostwald ripening) and coalescence between the droplets; and both can lead to the destabilization of the miniemulsion. Diffusional degradation is characterized by mass transfer of monomer from smaller to larger droplets and the coalescence occurs when two or more droplets are sufficiently close to permit their contact, thereby forming a single larger drop.

Figure 11. Coalescence and diffusional degradation schemes.

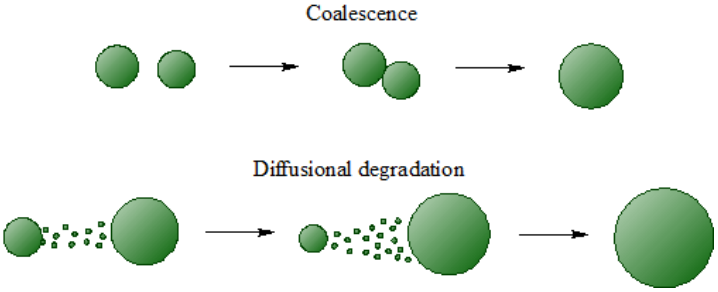

Source: Author.

To avoid coalescence, an effective surfactant must be added, promoting electrostatic and/or steric stabilization of the droplets (CHOU; EL-AASSER; VANDERHOFF, 1980). According to El-Aasser and Miller (1997), surfactants must satisfy the following requirements: (i) their structure must have polar and non-polar groups; (ii) they must be more soluble in aqueous phase and be readily available for adsorption on the droplets surface, (iii) they must adsorb strongly and not be easily displaced when two droplets collide; (iv) they must be effective at low concentrations; (v) they should be relatively inexpensive, non-toxic and safe to handle.

Diffusional degradation can be suppressed by the presence of a hydrophobic compound, called costabilizer, in the dispersed phase. According to Schork *et al.* (2005), the costabilizer retards the diffusion of monomer from smaller droplets to larger droplets and must have characteristics such as high solubility in the monomer, low solubility in water and low molecular weight. Costabilizers cannot be able to diffuse through the aqueous phase from one droplet to another; therefore, a difference in concentration of costabilizer inside the droplets, which increases with decreasing droplet size, creates a counterforce upon monomer diffusion. Thereafter, an osmotic pressure builds up and counteracts the Laplace pressure responsible for diffusional degradation (ANTONIETTI; LANDFESTER, 2002; ASUA, 2002; LANDFESTER, 2003; SCHORK *et al*., 2005). It is important to mention that the surfactant and costabilizer choice is a very important factor for the miniemulsion formulation because these compounds remain in the final polymer and may have a negative effect on the properties of the resulting latex.

Besides many possibilities for radical polymerization reactions in miniemulsion systems, other polymerization routes can be adapted to be

performed in miniemulsion, ranging from anionic, cationic and enzymatic polymerization to polyaddition and polycondensation (LANDFESTER; MUSYANOVYCH; MAILÄNDER, 2010).

2.4.1 ADMET and thiol-ene reactions in miniemulsion

There is a growing interest to perform metathesis and thiol-ene reactions in an aqueous phase aiming to work with an environmentally friendly system, but only few works were reported. Additionally, besides avoiding the use of organic solvents, the miniemulsion process enables the production of polymeric nanoparticles with unique characteristics and vast commercial interest - e.g. structured nanoparticles presenting different morphologies (LANDFESTER, 2009): hollow, hybrid, well-defined microstructure, and nanocapsules for inorganic solids (ROMIO *et al.*, 2013; STAUDT *et al.*, 2013) or drug encapsulation (BERNARDY *et al.*, 2010).

Pecher and Mecking (2007, 2010) performed aqueous miniemulsion polymerizations to obtain poly(phenylene-vinylene) conjugated nanoparticles by ADMET polymerization. This first attempt on producing polymer nanoparticles by ADMET miniemulsion polymerization resulted in polymers with very low molecular weights, M_n around 1.5kDa, using Grubbs 2nd generation and Hoveyda-Grubbs 2nd generation as catalysts and the cationic surfactant DTAC (dodecyltrimethylammonium chloride) for colloidal stabilization of the nanodroplets/polymeric nanoparticles. Although producing polymers with low molecular weights (below 2 kDa), these published studies have shown that carrying out metathesis reactions in miniemulsion may allow to obtain polymeric nanoparticles with microstructures inaccessible by other polymerization techniques (PECHER; MECKING, 2007).

Recently, Lobry *et al.* (2014) and Jasinski *et al.* (2014) reported the synthesis of poly(thioether) nanoparticles via thiol-ene reactions in miniemulsion using diallyl adipate and ethylene glycol dithiol as comonomers. The reactions performed via photopolymerization yielded polymers presenting a glass transition temperature (T_g) of -63 ºC and a melting temperature (T_m) of 18 ºC. Due to their high crystallinity, the polymers were insoluble in most of the organic solvents and, therefore, the authors presented the molecular weight only for the soluble part (M_n = 30 kDa).

Amato and coworkers (2015) also performed thiol-ene photopolymerization reactions in miniemulsion in order to obtain cross-linked poly(thioether) nanoparticles. The work investigated the effects

of surfactant concentration, organic phase/water phase ratio and the influence of a costabilizer in the miniemulsion. Furthermore, non-stoichiometric thiol-ene polymerization reactions were performed and nanoparticles presenting either thiol or ene functional groups on the surface were obtained.

The possibility of obtaining polymers containing water sensitive moieties, such as polyesters, in aqueous dispersed medium is a great advantage in performing ADMET and thiol-ene polymerization in miniemulsion. In addition, many other types of interesting materials could be obtained, e.g. nanocomposites, nanocapsules and hybrid particles. Moreover, polymers containing ester groups in the main chain can undergo hydrolysis, enabling its degradation in physiological environment, which is of major importance for biomedical applications or even the polymeric material disposal.

CHAPTER III

This chapter is part of a publication entitled "**ADMET reactions in miniemulsion**" published in the Journal of Polymer Science Part A: Polymer Chemistry, 52: 1300–1305, 2014.

3 ADMET REACTIONS IN MINIEMULSION

3.1 INTRODUCTION

Vegetable oils show a high potential as alternative resource for the production of polymeric materials because of their renewability, world wide availability, relatively low prices, and value added application possibilities. These advantages make them very attractive for the chemical industry, since their use could replace some petroleum based compounds (BELGACEM; GANDINI, 2008; MONTERO DE ESPINOSA; MEIER, 2011; MEIER, 2011; TÜRÜNÇ, MEIER, 2011). Furthermore, these renewable resources are considered to be very important for the production of biobased polymers due to, for example, their low toxicity and inherent biodegradability (BIERMANN *et al*., 2000; SHARMA; KUNDU, 2006; LLIGADAS *et al*., 2010).

Vegetable oils primarily consist of triacylglycerols (triglycerides). Fatty acids are 95% of the total weight of triglycerides and can be easily obtained by hydrolysis (or alcoholysis to obtain the respective esters). Depending on the fatty acid distribution, each type of oil has specific physical and chemical properties. Fatty acids have been studied as renewable building blocks for the synthesis of compounds with high added value and specific properties. Furthermore, often only a few minor modification reactions have to be performed prior to their application (MONTERO DE ESPINOSA; MEIER, 2011; GÜNER; YAĞCI; ERCIYES, 2006).

Since many fatty acids are unsaturated, metathesis generally is a successful and versatile tool to derivatise their double bonds in order to obtain new monomers and polymers (IVIN; MOL, 1997; MEIER; METZGER; SCHUBERT, 2007; RYBAK; FOKOU; MEIER, 2008; MEIER, 2009; BIERMANN *et al.,* 2011). In this context, the acyclic diene metathesis (ADMET) reaction is a promising technique to obtain high molecular weight polymers from renewable raw materials (MEIER; METZGER; SCHUBERT, 2007; RYBAK; FOKOU; MEIER, 2008; WARWEL et al., 2001; MUTLU; MONTERO DE ESPINOSA; MEIER, 2011; OPPER; WAGENER, 2011). The ADMET process has

been intensively studied since Wagener *et al.* (1990a; 1990b) reported the first examples of high molecular weight polymers obtained by polymerization of α,ω-dienes. ADMET polymerization follows a step-growth mechanism and is driven by the release of a low molecular weight condensate, usually ethylene. This metathesis reaction produces well-defined and strictly linear polymers with (modified) unsaturated polyethylene backbones (BAUGHMAN; WAGENER, 2005) and can only reach high molecular weights at high monomer conversion, like all traditional condensation polymerizations (MUTLU; MONTERO DE ESPINOSA; MEIER, 2011). Rybak *et al.* (2008) showed high molecular weight polymers (M_n up to 45 kDa) synthesized from undecylenyl undecenoate, a 100% castor-oil-derived monomer.

The synthesis of polymeric nanoparticles has been intensely investigated from a fundamental point of view to studies directed for specific applications (MEHNERT; MADER, 2001; TIARKS; LANDFESTER; ANTONIETTI, 2001; LANDFESTER, 2006; PECHER; MECKING, 2007; CAPEK, 2010; LANDFESTER; MUSYANOVYCH; MAILÄNDER, 2010). Nanoparticles are frequently obtained by free radical polymerization, where an organic phase is dispersed in an aqueous phase. In heterophase polymerization techniques, the synthesized polymer is not water-soluble and the monomer presents low solubility in water. Emulsion polymerization is a very well-established system used to synthesize polymeric nanoparticles.

On the other hand, miniemulsion polymerization has been earning importance in this field. The number of publications has increased and the development of novel polymeric materials obtained by this technique has become more common due to the combination of some attractive characteristics from conventional emulsion polymerization and the possibility of using and/or incorporating water insoluble reactants and compounds (EL-AASSER; MILLER, 1997; ASUA, 2002; ANTONIETTI; LANDFESTER, 2002; SCHORK *et al.*, 2005), such as several vegetable oils (CARDOSO; ARAUJO; SAYER, 2013). Therefore, the miniemulsion process enables the production of polymeric nanoparticles with unique characteristics and vast commercial interest - e.g. structured nanoparticles presenting different morphologies (LANDFESTER, 2009): hollow, hybrid, well-defined microstructure, and nanocapsules for inorganic solids (ROMIO *et al.*, 2013; STAUDT *et al.*, 2013) or drug encapsulation (BERNARDY *et al.*, 2010).

There is a growing interest to perform metathesis reactions in an aqueous phase aiming to work with an environmentally friendly system,

but only few works were reported. For example, Lynn *et al.*(1996) investigated living ROMP reactions of norbornene derivatives in aqueous emulsion and Pecher and Mecking (2007; 2010) performed aqueous miniemulsion polymerizations to obtain poly(phenylenevinylene) conjugated nanoparticles by ADMET polymerization. This first attempt on producing polymer nanoparticles by ADMET miniemulsion polymerization resulted in polymers with very low molecular weight, 1.5 kDa, using Grubbs 2nd generation and Hoveyda-Grubbs 2nd generation as catalysts and a cationic surfactant (dodecyltrimethylammonium chloride, DTAC) for colloidal stabilization of the nanodroplets/polymeric nanoparticles. The absence of organic solvents in ADMET reactions in miniemulsion afforded polymeric nanoparticles with microstructures inaccessible by other polymerization techniques (PECHER; MECKING, 2007).

Therefore, this Chapter aims to contribute to the study of ADMET reactions in aqueous miniemulsion polymerization evaluating different types of catalysts and different surfactants (anionic, cationic and non-ionic). A set of ADMET polymerizations of 1,3-propylene diundec-10-enoate (Figure 12), a diester monomer derived from castor oil, was used to evaluate the performance of different types of ruthenium-based catalyst (Hoveyda Grubbs 2nd generation, Grubbs 1st generation and Umicore M2) and surfactants (sodium dodecyl sulfate - SDS, cetyltrimethylammonium bromide - CTAB, and Lutensol AT80, which is a $C_{16}C_{18}$ fatty alcohol ethoxylate with 80 ethylene oxide units).

Figure 12. ADMET polymerization reaction of the studied α,ω-diene (1,3-Propylene Diundec-10-enoate).

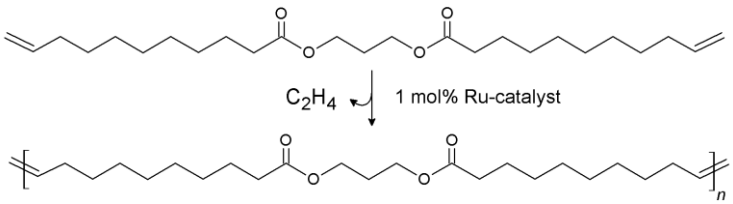

Source: Author.

3.2 EXPERIMENTAL PROCEDURE

3.2.1 Materials

10-Undecenoic acid (Sigma-Aldrich, 98%), 1,3-propanediol (Sigma-Aldrich, 99.6%), p-toluenesulfonic acid monohydrate (Sigma-Aldrich, 98.5%), ethyl vinyl ether (Sigma-Aldrich, 99%), sodium dodecyl sulfate (SDS, Sigma-Aldrich, 99%), cetyltrimethylammonium bromide (CTAB, Sigma-Aldrich, 98%), Lutensol AT80 (BASF), which is a $C_{16}C_{18}$ fatty alcohol ethoxylate with 80 ethylene oxide units (molecular weight ca. 3.8kDa). The catalysts used were (1,3-bis(2,4,6-trimethylphenyl)-2-imidazolidinylidene)dichloro(o-isopropoxyphenyl-methylene)ruthenium (II) (Hoveyda-Grubbs catalyst 2nd generation, HG2, Sigma-Aldrich), benzylidene-bis(tricyclehexylphosphine) dichlororuthenium (Grubbs catalyst, 1st generation, G1, Sigma-Aldrich), [1,3-bis(2,4,6-trimethylphenyl)-2-imidazolidinylidene]dichloro-(3-phenyl-1H-inden-1-ylidene)(tricyclohexylphosphine)ruthenium(II) (Umicore M2, UM2, Umicore), shown in Figure 13. All materials were used as received. Distilled water was used in all experiments.

Figure 13. Catalysts used in the ADMET reactions in miniemulsion. a) Hoveyda Grubbs 2nd generation (HG2); b) Grubbs 1st generation (G1); c) Umicore M2 (UM2).

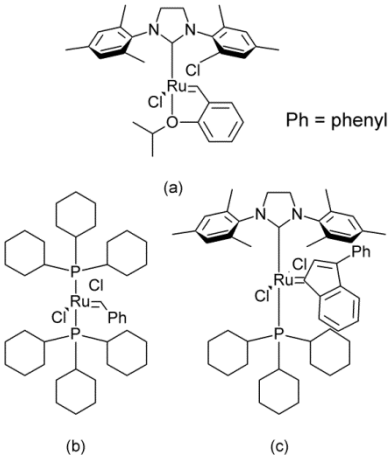

Source: Author.

3.2.2 Monomer synthesis

10-Undecenoic acid (50.0 g, 0.27 mol), 1,3-propanediol (8.4 g, 0.11 mol), p-toluenesulfonic acid (3 g, 0.0157 mol) and toluene (200 mL) were added to a round-bottomed flask equipped with a magnetic stirrer and a Dean-Stark apparatus. The resulting mixture was heated to reflux and water was collected as the reaction proceeded. Once the reaction was completed, the reaction mixture was allowed to cool down. Figure 14 shows a scheme of the esterification reaction. After removing the toluene under reduced pressure, the residue was filtered through a short pad of basic aluminium oxide with hexane as eluent. Hexane was removed and the crude product was dissolved in diethyl ether (200 mL) and washed two times with water (200 mL). The organic fraction was dried over anhydrous MgSO4 and the solvent removed under reduced pressure. The desired product was isolated in 78% yield (35.2 g) and analyzed by 1H NMR and 13C NMR spectroscopy.

^{1}H NMR (300 MHz, $CDCl_3$, δ): 5.85–5.76 (m, 2H, 2x-CH=CH_2), 5.00–4.91 (m, 4H, 2xCH=CH_2), 4.15 (t, 4H, J=6.1 Hz, 2xCH_2OCO-), 2.30 (t, 4H, J = 7.3 Hz, CH_2COO-), 2.00 (m, 4H, 2xCH_2-CH=CH_2), 1.99–1.94 (m, 2H, J = 6.1 Hz, CH_2CH_2OCO-), 1.64–1.58 (m, 4H, 2xCH_2CH_2COO-), 1.38–1.34 (m, 4H, 2xCH_2) 1.29–1.24 (br.s, 16H, 2x[4CH_2]) ppm. ^{13}C NMR (600 MHz, $CDCl_3$, δ): 173.6 (s, -COO-), 139.0 (s, -CH=CH_2), 114.1 (s, -CH=CH_2), 60.7 (s, CH_2OCO-), 34.1 (s, CH_2), 33.7 (s, CH_2), 29.2 (s, CH_2), 29.1 (s, CH_2), 29.0 (s, CH_2), 28.8 (s, CH_2), 24.8 (s, CH_2) ppm. MS (EI): m/z = 408 [M]+, calc. 408.3239.

Figure 14. Esterification reaction of 10-undecenoic acid and 1,3-propanediol to yield 1,3-propylene diundec-10-enoate.

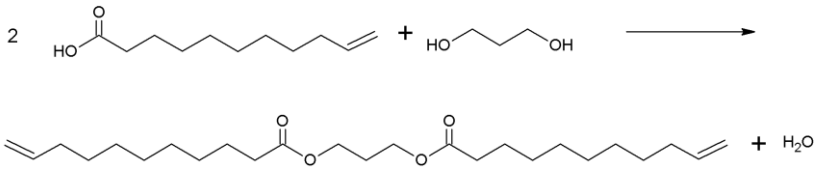

Source: Author.

3.2.3 ADMET polymerization reactions

For the miniemulsion reactions, 2 pre-emulsions were prepared, the first one (1) mixing water (2 mL) and surfactant with chloroform (0.25 g) and catalyst (1 mol% related to monomer) and the second (2) mixing water (8 mL) and surfactant with monomer (1 g). After 20 min of magnetic stirring, 1 and 2 were sonicated separately (Branson Ultrasonics Corp., Branson Digital Sonifier W450) for 1 min with an amplitude of 60%, using a ½" tip. Then, the miniemulsions were mixed and sonicated again for 2 more minutes. An ice bath was used to reduce the temperature increase during the sonication. In the case where bulk reactions were performed, monomer (1 g) and 1 mol% of the catalyst were mixed at the reaction temperature.

Figure 15 shows the schematic representation of the procedure adopted for the miniemulsion reactions. At first, two different attempts were performed adding the catalyst directly to the monomer before and during the sonication. However, in both cases, the resulting miniemulsion was not stable.

Figure 15. Schematic representation of ADMET reactions in miniemulsion.

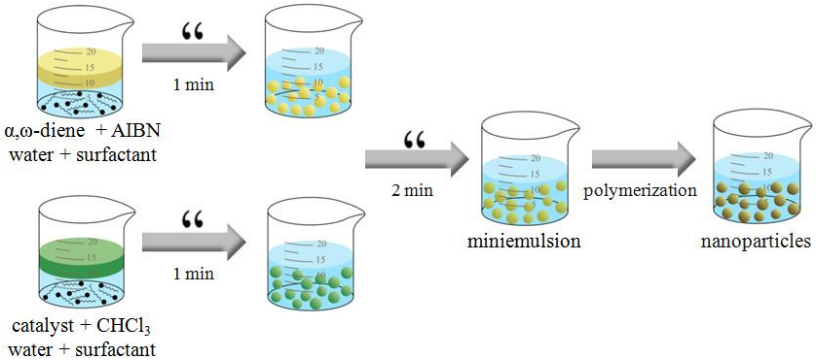

Source: Author.

Batch polymerization reactions were carried out in 3 mL conical vials (Supelco) equipped with screw cap and septum and the mixtures were stirred at the desirable temperature. After 6 h, the reactions mixtures were diluted in THF and polymerization halted with excess of ethyl vinyl ether and stirring for 30 min at room temperature. The

residue was precipitated into cold methanol for polymer isolation by filtration and subsequent polymer analysis.

3.2.4 Particle Size Measurements

Intensity average diameters of the polymer particles (Dp) and the polydispersity indexes (PDI) were measured by dynamic light scattering (DLS - Malvern Instruments, Zeta SizerNano S). The latex samples were diluted approximately 1:15 with distilled water prior to DLS analysis.

3.2.5 Molecular weight

Molecular weight distributions were determined using a Shimadzu SEC System LC-20 A equipped with a SIL-20A auto sampler, GPC pre-column PSS SDV analytical (5 µm, 8×50 mm), main-column PSS SDV analytical 10000 Å (5 µm, 8×300 mm) and a RID-10A refractive index detector in THF (flow rate 1 mL×min^{-1}) at 50 °C. The molecular weight distributions were determined relative to PMMA standards (Polymer Standards Service, Mp 1100 – 981000 Da).

3.2.6 Nuclear Magnetic Resonance

^{1}H NMR and ^{13}C NMR spectra were recorded in $CDCl_3$ on Bruker AVANCE DPX spectrometers operating at 300 and 600 MHz. Chemical shifts (δ) are reported in parts per million relative to the internal standard tetramethylsilane (TMS, δ = 0.00 ppm).

3.2.7 Differential scanning calorimetry

DSC experiments were carried out under a nitrogen atmosphere (30 mL min^{-1}) at a heating rate of 10 °C min^{-1} on a Mettler Toledo DSC 823 calorimeter. The melting temperature, T_m, was recorded from the second heating ramp from -50 ºC to 180 ºC.

3.3 RESULTS AND DISCUSSION

To start our investigations, the α,ω-diene monomer 1,3-propylene diundec-10-enoate was prepared by a procedure found in the literature (MUTLU *et al.*, 2010b) using 1,3-propanediol, which can be prepared from glycerol by fermentation, and 10-undecenoic acid, a commercial derivative of castor oil and an important raw material for cosmetics, pharmaceuticals, and polymeric compounds (MUTLU *et al.*, 2010a). ADMET polymerizations of the 100% renewable monomer were performed to study the effect of the catalyst and the surfactant type at different temperatures (45 and 85 °C), under miniemulsion (Mini) and bulk (B) conditions, after 6 h reaction time and the results are shown in Table 2.

The reactions resulted in particle sizes in the range of 150-350 nm, depending on the type of surfactant employed. The amount of SDS and CTAB were fixed to 0.3 wt.% related to water and the non-ionic Lutensol was fixed to 3.0 wt.%. The weight fraction difference between the surfactants is due to the much higher molecular weight of Lutensol AT80 (~3.8 kDa).When comparing the mole fraction of the surfactants related to water, Lutensol and CTAB present almost the same mol fraction, 0.014 and 0.015 mol%, respectively. Although SDS presented the higher mol fraction, 0.019 mol%, the stabilization of the monomer droplets was less effective, with an average diameter around 300 nm and highly disperse particle size distribution (PDI superior to 0.2). SDS is usually a very effective surfactant, but our results indicate that there was an interaction between the SDS and the catalyst HG2 decreasing the stabilization efficiency of SDS and the catalyst activity.

A first set of experiments (Table 2, entries 1 and 2) showed that no polymerization occurred when employing the HG2 catalyst in the presence of the anionic sodium dodecyl sulfate (SDS) at either 45 or 85 °C. A similar behavior was observed by Pecher and Mecking (2007) using SDS to polymerize 1,4-dipropoxy-2,5-divinylbenzene by ADMET polymerization in aqueous miniemulsion using Grubbs 2nd generation and HG2 as catalyst, where no polymerization occurred. It has also been reported by Lynn and coworkers (1996) that low yields of polynorbornene were produced by living ROMP using G1 as catalyst and the anionic surfactant SDS. Higher yields were achieved when changing to the cationic surfactant DTAB (dodecyltrimethylammonium bromide) in this case.

Table 2. Formulation and results of ADMET polymerization of 1,3-Propylene Diundec-10-enoate. Catalyst type (Cat), process conditions (miniemulsion or bulk), temperature, surfactant type (SDS, CTAB or Lutensol AT80), average particles diameter (Dp), polydispersity index (PDI), number average molecular weight (M_n) and weight average molecular weight (M_w).

Entry	Cat	Process[a]	Temp (ºC)	Surf.[b]	Dp[c] (nm)	PDI	M_n (kDa)[d]	M_w (kDa)[d]
1	HG2	Mini	45	SDS	329	0.25	-	-
2	HG2	Mini	85	SDS	349	0.29	-	-
3	HG2	Mini	45	CTAB	156	0.12	1.0	1.5
4	HG2	Mini	85	CTAB	192	0.16	2.2	2.6
5	HG2	B	85	-	-	-	4.5	8.6
6	HG2	Mini	85	Lut80	243	0.15	2.7	4.0
7	G1	Mini	85	CTAB	186	0.16	1.2	2.0
8	G1	Mini	85	Lut80	212	0.17	1.4	2.1
9	G1	B	85	-	-	-	2.0	3.4
10	UM2	Mini	85	CTAB	169	0.14	7.2	15.1
11	UM2	Mini	85	Lut80	302	0.12	14.7	26.5
12	UM2	B	85	-	-	-	4.7	9.4

[a] Process condition: miniemulsion (Mini) or bulk (B).[b] surfactant type. [c] average particle diameter obtained by DLS; [d] GPC was performed in THF with PMMA calibration.

Reactions using the cationic cetyltrimethylammonium bromide (CTAB) as surfactant (Table 2, entries 3 and 4) showed that the CTAB did not deactivate the catalyst (HG2), as SDS did. However, lower molecular weights were obtained when compared to a bulk reaction (Table 2, entry 5). It should be mentioned here that no efforts were taken to remove the ethylene from this bulk reaction (i.e vacuum or inert gas flow) in order to make the results more comparable to the miniemulsion reactions. Of course, much higher molecular weights can be achieved, if such experimental set-ups are chosen. In any case, these results may be

attributed to partial HG2 catalyst decomposition in water (PECHER; MECKING, 2007). Increasing the reaction temperature from 45 to 85°C resulted in some increase in the molecular weight due the increased catalyst activity (MUTLU *et al*., 2010b)

The effect of the catalysts type (G1, HG2, UM2) in miniemulsion was investigated under similar conditions in terms of concentrations of reagents in the organic phase and temperature (Table 1, entries 4, 7 and 10) using CTAB as surfactant. The molecular weight distribution was analyzed by GPC (Figure 16). The number average molecular weight, M_n, of the resulting polymer followed the order UM2 (~7 kDa) >> HG2 (~2 kDa) > G1 (~1 kDa). This result is in accordance with previous works that showed that all indenylidene Ru-catalysts, like UM2, were more robust under similar reaction conditions compared to their Ru-benzylidene counterparts, like G1 and HG2 (MUTLU *et al*., 2010b; BURTSCHER *et al*., 2008; MONSAERT *et al*., 2008; ADEKUNLE *et al*., 2010).

Figure 16. GPC traces of ADMET polymerizations in miniemulsion performed with HG2 (P4), G1 (P7) and UM2 (P10) as catalyst and CTAB as surfactant.

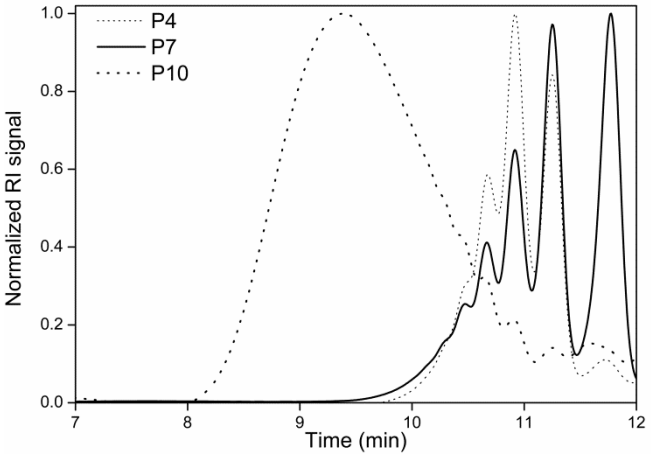

Reactions using the non-ionic surfactant Lutensol AT80 with different catalysts (Table 2, entries 6, 8 and 11) produced polymers with higher molecular weight (Figure 17) by comparison to the reactions using the same catalyst but with the cationic surfactant CTAB (Table 2, entries 4, 7 and 10; Figure 16). This effect is more pronounced when comparing the polymers P10 (M_n= ~7 kDa) and P11 (M_n= ~15 kDa), obtained with CTAB and Lutensol AT80, respectively, and UM2 as

catalyst. The higher reactivity observed in the reactions with the non-ionic surfactant indicates that the electronic charge of the surfactants affected the catalyst activity, although the cationic surfactant did not deactivate the catalyst to the same extent as the anionic surfactant did.

DSC results (Figure 18) showed that polymer P11 (Table 2, entry 11), obtained with UM2 and Lutensol AT80, exhibited a quite sharp T_m peak at 30.0 °C, indicating a higher structural regularity by comparison to polymer P10 (Table 2, entry 10), obtained with UM2 and CTAB, which presented a broader melting transition peak probably because of its broader molecular weight distribution with peaks of low molecular weight polymer.

Figure 17. GPC traces of ADMET polymerizations in miniemulsion performed with HG2 (P6) and UM2 (P11) as catalysts and Lutensol AT80 as surfactant.

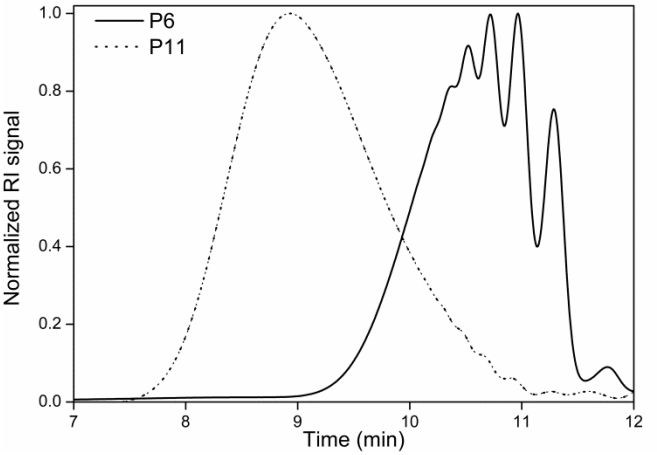

The molecular weight of the reaction performed in miniemulsion using the catalyst UM2 and Lutensol AT80 as surfactant (Table 2, entry 11) was more than three times higher than the molecular weight of the reaction in bulk (Table 2, entry 12). Apparently, the much higher surface area of the organic phase in miniemulsion polymerization improved the release of the ethylene formed during the metathesis reaction from the polymer particles as the bulk reaction was performed without any attempt, such as vacuum or nitrogen flow, to remove the ethylene from the reaction medium. Therefore, results showed that using Umicore M2 and the non-ionic Lutensol AT80 resulted in the highest molecular weight obtained in the present work.

Figure 18. DSC traces of ADMET polymers P10 and P11.

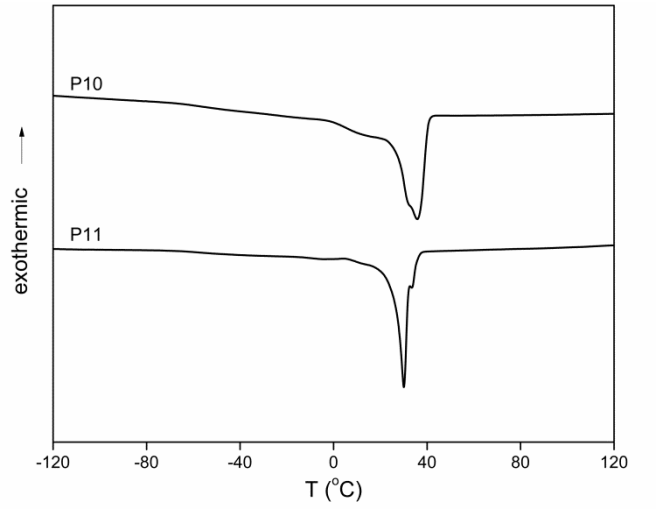

3.4 CONCLUSION

ADMET reactions were successfully performed in miniemulsion. The studied process produced polymers with weight average molecular weight up to 15 kDa (M_n), depending on the catalyst and the surfactant employed. The Ru-indenylidene catalyst, UM2, has presented higher activity in water by comparison to the Ru-benzylidene catalysts, G1 and HG2. In addition, the catalysts activity was significantly affected by the type of the surfactant. The large surface area of the organic phase in miniemulsion probably enhanced ethylene removal from the reaction locus, promoting ADMET polymerization and achieving higher molecular weights than in bulk. Moreover, Umicore M2 catalyst and the surfactant Lutensol AT80 were found to be the most suitable combination for ADMET reactions in miniemulsion polymerization.

CHAPTER IV

This chapter is part of a publication entitled "**Biobased polymeric nanoparticles from castor oil derivatives by thiol-ene miniemulsion polymerization**" under submission.

4 THIOL-ENE REACTIONS IN MINIEMULSION

4.1 INTRODUCTION

Thiol-ene polymerization is considered as a click-chemistry reaction because it can be carried out under mild conditions and normally provides a high yielding and generation of inoffensive by-products (HOYLE; LEE; ROPER, 2004; HOYLE; BOWMAN, 2010). In addition, thiol-ene reaction has been shown as a versatile tool to produce polymers from fully renewable α,ω-diene monomers bearing, for example ester, ether, or amide functional groups in the backbone chain (FIRDAUS; MONTERO DE ESPINOSA; MEIER, 2011; TÜRÜNÇ, 2012; TÜRÜNÇ; MEIER, 2013).

There is a growing interest in developing novel biomaterials aiming applications in drug delivery systems, tissue engineering and environmental issues. In this context, thiol-ene reactions have been earning attention due to the improved mechanical properties, unique crosslinking structure and tunable degradability behavior provided by these click reactions (KADE; BURKE; HAWKER, 2010; HOYLE; LOWE; BOWMAN, 2010; REDDY; ANSETH; BOWMAN, 2005). Moreover, thiol-ene mechanism provides clean and environmentally harmless reactions, without using organic solvents and toxic metal catalysts, which are commonly employed in other "click" reactions and also in metathesis reactions (such as ADMET).

Apart from the advantages already mentioned, thiol-ene reactions allow the synthesis of high molecular weight polyesters in aqueous dispersed medium and thereby are suitable for the production of polymeric nanoparticles containing ester groups in the main chain, which can undergo hydrolysis, enabling their degradation in physiological environment, which is of great importance for biomedical applications or material disposal (JASINSKI *et al.*, 2014; MACHADO; SAYER; ARAÚJO, 2016).

Besides avoiding the use of organic solvents, miniemulsion polymerization possesses some advantages over other types of polymerization such as bulk and solution polymerizations, because it

yields products with low viscosity and therefore mass, heat and momentum transfer is improved. Additionally, the miniemulsion process enables the production of polymeric nanoparticles with unique characteristics and vast commercial interest (EL-AASSER; MILLER, 1997; ASUA, 2002; ANTONIETTI; LANDFESTER, 2002). Thiol-ene step-growth polymerization in miniemulsion is being currently investigated and only a handful of articles have been published in the literature (JASINSKI *et al.*, 2014; LOBRY *et al.*, 2014; AMATO *et al.*, 2015; MACHADO *et al.*, 2016). Furthermore, works portraying the polymerization of renewable monomers through thiol-ene polymerization in aqueous dispersed medium are still uncommon.

Herein, it is presented the synthesis and characterization of poly(thioether-ester) nanoparticles via thiol-ene polymerization in miniemulsion using a fully renewable α,ω-diene monomer (derived from castor oil and glycerol). Furthermore, little is known about the reactivity of different diene monomers in thiol-ene reactions, especially in the presence of water. Thus, the goal of this chapter is to provide basic information regarding this matter.

4.2 EXPERIMENTAL PROCEDURE

4.2.1 Materials

10-Undecenoic acid (Sigma-Aldrich, 98%), 1,3-propanediol (Sigma-Aldrich, 99.6%), p-toluenesulfonic acid monohydrate (Sigma-Aldrich, 98.5%), sodium dodecyl sulfate (SDS, Sigma-Aldrich, 99%), 1,4-butanedithiol (Sigma-Aldrich, >97%), 2-mercaptoethyl ether (Sigma-Aldrich, 95%), 4-pentenoic acid (Sigma-Aldrich, 97%), 1,7-octadiene (Sigma-Aldrich, 98%), Lutensol AT80 (BASF), which is a $C_{16}C_{18}$ fatty alcohol ethoxylate with 80 ethylene oxide units (molecular weight ca. 3.8 kDa). All materials were used as received. Distilled water was used in all experiments.

4.2.2 Monomer synthesis

The 100% renewable α,ω-monomer 1,3-propylene diundec-10-enoate was prepared following the procedure described in Chapter 3, session 3.2.2.

For the short α,ω-diene diester monomer, 4-pentenoic acid (27.0 g, 0.27 mol), 1,3-propanediol (8.4 g, 0.11 mol), p-toluenesulfonic acid (3 g, 0.0157 mol) and toluene (200 mL) were added to a round-

bottomed flask equipped with a magnetic stirrer and a Dean-Stark apparatus. The resulting mixture was heated to reflux and water was collected as the reaction proceeded. Once the reaction was completed, the reaction mixture was allowed to cool. Figure 19 shows a scheme of the esterification reaction. After removing the toluene under reduced pressure, the residue was filtered through a short pad of basic aluminium oxide with hexane as eluent. Hexane was removed and the crude product was dissolved in diethyl ether (200 mL) and washed two times with water (200 mL). The organic fraction was dried over anhydrous $MgSO_4$ and the solvent removed under reduced pressure. The desired product was isolated in 62% yield (16.4 g) and analyzed by ^{1}H NMR (Figure 20) and ^{13}C NMR spectroscopy.

Figure 19. Esterification reaction of 4-pentenoic acid and 1,3-propanediol to yield 1,3-propylene dipent-4-enoate.

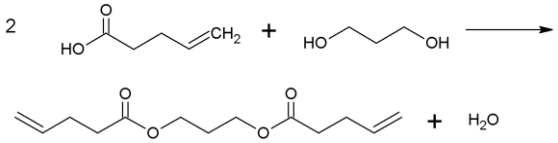

Source: Author.

Figure 20. ^{1}H NMR spectrum of 1,3-propylene dipent-4-enoate (monomer M2). Peaks labelled and match to the hydrogen atoms in the molecule.

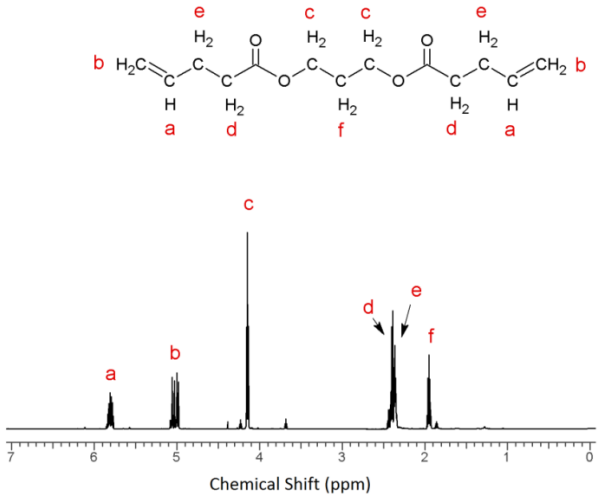

^{1}H NMR (600 MHz, $CDCl_3$, δ): 5.79–5.73 (m, 2H, 2x-CH=CH_2), 5.02–4.94 (m, 4H, 2xCH=CH_2), 4.10 (t, 4H, J=6.3 Hz, 2xCH_2OCO-), 2.40-2.35 (m, 4H, J = 7.3 Hz, CH_2COO-), 2.33-2.31 (m, 4H, 2xCH_2-CH=CH_2), 1.93–1.89 (m, 2H, J = 6.1 Hz, CH_2CH_2OCO) ppm. ^{13}C NMR (600 MHz, $CDCl_3$, δ): 173.0 (s, -COO-), 136.6 (s, -CH=CH_2), 115.5 (s, CH=CH_2), 60.9 (s, CH_2OCO-), 33.4 (s, CH_2), 28.8 (s, CH_2), 27.9 (s, CH_2) ppm. [M] calc.: 240.2955.

4.2.3 Thiol-ene polymerization reactions

For the miniemulsion reactions, the aqueous phase was prepared mixing water (10 mL) and the surfactant SDS (wt. %) and the mixture was let stirring until complete surfactant solubilization. The organic phase was prepared mixing α,ω-diene monomer (1.0 g) and, if used, organic-soluble initiator (AIBN) under magnetic stirring until complete initiator solubilization. The aqueous phase was added to the organic phase and, after 10 min of vigorous magnetic stirring (500 rpm), a pre-emulsion was obtained. Then the dithiol was added to the system (1:1 dithiol-to-diene molar ratio) with a micropipette and the mixture was let under mild magnetic stirring (250 rpm) for 5 minutes. The final emulsion was sonicated for 2 minutes with amplitude of 60% in a pulse regimen (10 seconds of sonication, 2 seconds of pause), using a Branson Digital Sonifier model W450 and a ½" tip. An ice bath was used to reduce the temperature increase during the sonication.

Figure 21 shows the schematic representation of the procedure adopted for the miniemulsion reactions.

Figure 21. Schematic representation of thiol-ene reactions in miniemulsion.

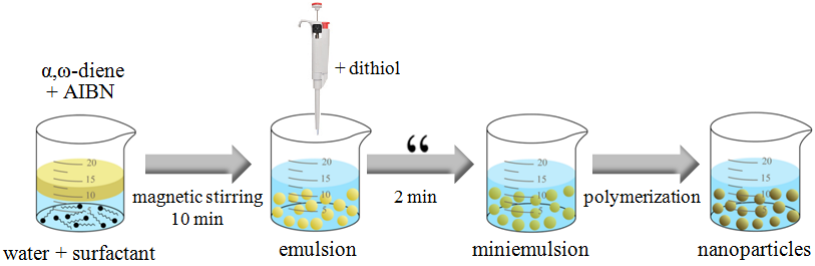

Source: Author.

In the case where bulk reactions were performed, diene monomer (1 g) and organic-soluble initiator (AIBN) were mixed at room

temperature and, after complete initiator solubilization, dithiol was added to the system (1:1 dithiol-to-diene molar ratio).

Batch polymerization reactions were carried out in 3 mL conical vials (Supelco) equipped with screw cap and septum and the mixtures were stirred at 80 ºC. After 3 h, the reactions mixtures were diluted in THF and the residue was precipitated into cold methanol for polymer isolation by filtration and subsequent polymer analysis.

4.2.4 Particle Size Measurements

Intensity average diameters of the polymer particles (Dp) and the polydispersity indexes (PDI) were measured by dynamic light scattering (DLS - Malvern Instruments, Zeta SizerNano S). The latex samples were diluted approximately 1:15 with distilled water prior to DLS analysis.

4.2.5 Molecular weight

Molecular weight distributions were determined using a Shimadzu SEC System LC-20 A equipped with a SIL-20A auto sampler, GPC pre-column PSS SDV analytical (5µm, 8×50mm), main-column PSS SDV analytical 10000 Å (5 µm, 8×300mm) and a RID-10A refractive index detector in THF (flow rate 1 mL×min^{-1}) at 50 °C. The molecular weight distributions were determined relative to PMMA standards (Polymer Standards Service, Mp 1100 - 981000 Da).

4.2.6 Nuclear Magnetic Resonance

^{1}H NMR and ^{13}C NMR spectra were recorded in $CDCl_3$ on Bruker Ascend 600 spectrometer operating at 600 MHz. Chemical shifts (δ) are reported in parts per million relative to the internal standard tetramethylsilane (TMS, δ = 0.00 ppm). Analyses were performed at the Laboratório de Ressonância Magnética Nuclear – LRMN, University of Brasília – UnB, Brazil.

4.2.7 Differential scanning calorimetry

DSC experiments were carried out under a nitrogen atmosphere (30 mL min-1) at a heating rate of 10 °C min^{-1} on a Mettler Toledo DSC 823 calorimeter. The melting temperature, T_m, was recorded from the

second heating ramp, from -50 ºC to 180 ºC.

4.2.8 Transmission Electron Microscopy (TEM)

Particle morphology characterization was performed by Transmission Electron Microscopy using a JEM-1011 TEM (100 kV). For this analysis, the sample was diluted in distilled water down to 0.01% of solids content and one single drop was placed on a carbon-coated copper grid. Then the grid was dried under room conditions overnight. These analyses were performed in the Laboratório Central de Microscopia Eletrônica (LCME), Federal University of Santa Catarina.

4.2.9 Fourier Transform Infrared Spectroscopy (FTIR)

Attenuated Total Reflectance Fourier Transform Infrared (ATR-FTIR) spectroscopy was performed on a Bruker spectrometer, model TENSOR 27, in the range of wavenumbers 4000-600 cm^{-1} by accumulating 32 scans at a resolution of 4 cm^{-1}. The polymer samples were analyzed (as powder) in the Laboratório de Materiais (LABMAT) at the Mechanical Engineering Department of the Federal University of Santa Catarina.

4.3 RESULTS AND DISCUSSION

To start our studies, three different α,ω-diene monomers (M1, M2, M3) and two different dithiols (BDT and MEE) with different chain lengths and functional groups (Figure 22) were chosen to perform thiol-ene polymerization reactions under miniemulsion and bulk conditions. M1 (1,7-octadiene) is commercially available and is obtained from non-renewable resources. This monomer does not present any ester group and therefore the polymer derived from this monomer does not undergo hydrolysis. M2 and M3, both α,ω-diene diester monomers, were synthesized by a esterification procedure using 1,3-propanediol; M2 was prepared using 4-pentenoic acid and M3, using 10-undecenoic acid.

Figure 22. Monomers used in the thiol-ene polymerization reactions. 1,7-Octadiene (M1), 1,3-propylene dipent-4-enoate (M2), 1,3-propylene diundec-10-enoate (M3), 1,4-butanedithiol (BDT) and 2-mercaptoethyl ether (MEE).

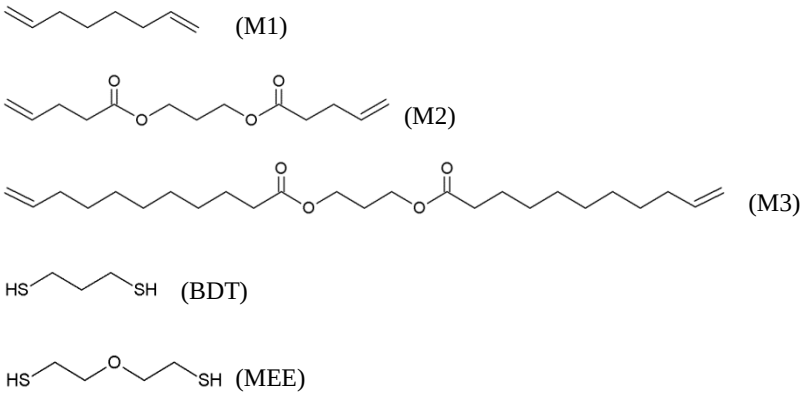

Source: Author.

In the first experiments (Table 3), a set of reactions was performed in bulk to verify the effect of initiator concentration on the molecular weight. The experiments were carried out at 80 ºC for 3 h and 1,4-butanedithiol was employed as comonomer. For all reactions the yielding based on monomer consumption (quantified by gravimetry and ^{1}H NMR analyses) was higher than 99% as usually occur in step-growth polymerization.

Table 3.Formulation and results of thiol-ene polymerization of different diene monomers and 1,4-butanedithiol. Monomer type, AIBN concentration, number average molecular weight (M_n) and weight average molecular weight (M_w).

Entry	Diene monomer	[AIBN] (mol%)	M_n (kDa)[a]	M_w (kDa)[a]
B1	M1	0.25	4.3	8.6
B2	M1	0.5	4.2	8.4
B3	M1	1.0	4.3	8.2
B4	M2	0.25	4.8	9.1
B5	M2	0.5	4.9	9.8
B6	M2	1.0	5.0	10.0
B7	M3	0.25	5.4	15.1
B8	M3	0.5	8.4	28.6
B9	M3	1.0	17.6	33.4
B10	M3	1.5	19.6	38.3

[a]GPC was performed in THF with PMMA calibration.

Reactions using 1,7-octadiene (B1, B2, B3) showed no difference when the amount of the initiator AIBN was increased from 0.25 to 0.5 and 1 mol% (related to the dithiol), resulting in number average molecular weight, M_n, around 4.3 kDa. When using the monomer 1,3-propylene dipent-4-enoate (B4, B5, and B6), reactions presented the same behavior, resulting in M_n around 5 kDa, regardless of initiator concentration. On the other hand, reactions using 1,3-propylene diundec-10-enoate (B7, B8, B9 and B10) showed an increase in the molecular weight when increasing the initiator concentration (Figure 23). Generally, molecular weight in radical polymerization drifts to lower values with the increase in initiator concentration (ODIAN, 2009); in thiol-ene polymerization, however, this behavior was not observed. One possible reason is the unique mechanism of thiol-ene polymerization, based on two main steps: the addition of a thiyl radical across the ene double bond followed by the electron transfer from the carbon centered radical to a thiol group. Therefore, molecular weight in thiol-ene polymerization is more likely

to depend on functional group conversion than on initiator concentration.

Figure 23. GPC traces of poly(thioether-ester) samples obtained using monomer M3 under different concentrations of AIBN.

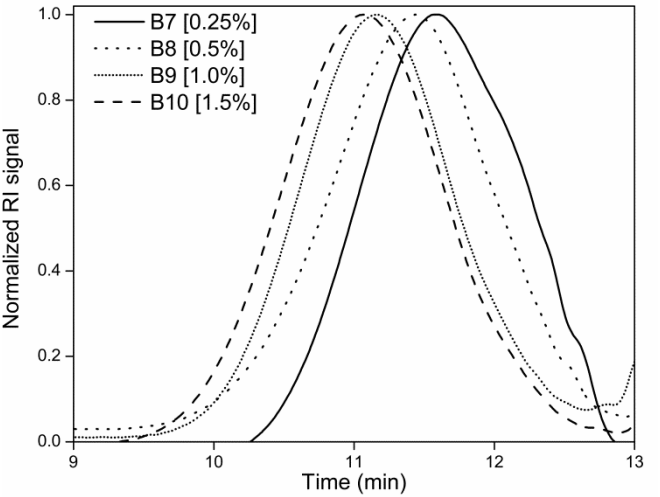

Comparing the three monomers, only thiol-ene polymerization with 1,3-propylene diundec-10-enoate (M3) had an increase in molecular weight with the increase of initiator. This might be due to the difference in kinetics intrinsically attained to different types of monomeric structures. It is likely that the thiol-ene polymerization kinetics with both M1 and M2 monomers are faster than with monomer M3, and thus achieving in shorter reaction times, or lower initiator amounts, high degrees of polymerization up to the maximum. At functional group conversion limit due to kinetic issues, such as low mobility of polymeric chains, there is no increase in molecular weight. Thus possibly monomers M1 and M2 reached the degree of polymerization limit, the functional group conversion limit, regardless initiator concentration, whilst monomer M3 possess a slower polymerization kinetics and presents an increase in degree of polymerization, i.e. molecular weight, with the increase of initiator concentration. Polymers with monomer M3 reached higher molecular weight (Figure 24) because 1,3-propylene diundec-10-enoate has a higher molecular weight (408.3 Da) than 1,7-octadiene(110.2 Da) and 1,3-propylene dipent-4-enoate (240.3 Da) (see Figure 22). This

explanation based on the monomer's molecular weight can be further confirmed when the polymerization reactions with monomers M1 and M2 are compared, even though there is only a slight difference in the polymers' molecular weight.

Figure 24.GPC traces of poly(thioether) samples obtained using 0.5 mol% of AIBN and different types of diene monomers (M1, M2 or M3).

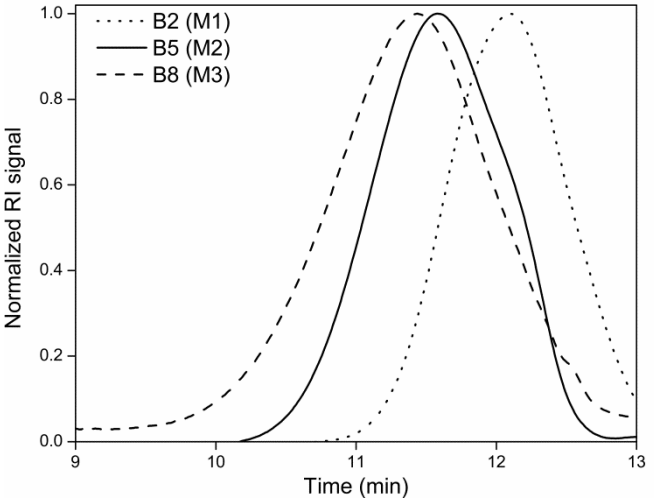

The melting point (T_m) of polymeric samples was checked by differential scanning calorimetry (DSC) and results are displayed in Figure 25. As observed, the synthesized poly(thioether)s presented sharp melting endotherms, a characteristic of semicrystalline polymers, similar to other thioether containing polyesters. This phenomenon for thioether containing homopolyesters was already mentioned and attributed to melting and recrystallization processes occurring during the calorimetric run (LOTTI *et al*., 2006). Figure 25 also reveals a variation of the T_m from 42 ºC to 72 ºC, depending on the diene monomer copolymerized with 1,4-butanedithiol; the higher T_m of B9 is due to the longer chain length of M3 (if compared to M1 and M2) and a more regular structure of the polymer (spacing of the ester groups), both allowing a better crystallization of B9. In addition, the polymers exhibited double melting endotherms revealing that the polymers first undergo a melting process causing an increase in chain mobility and leading to a crystallization, which is followed by a second melting (YU *et al*., 1983; TÜRÜNÇ, MEIER, 2010).

It is important to mention that the glass transition temperature of the polymers was not possible to observe by DSC analysis due to their crystallinity; however, the T_g could be determined by relaxation methods such as dynamic mechanical and dielectric spectroscopies (FOCARETE *et al.*, 2001).

Figure 25. DSC traces of poly(thioether) samples obtained in bulk with M1 (B3), M2 (B6) or M3 (B9) using 1 mol% of AIBN.

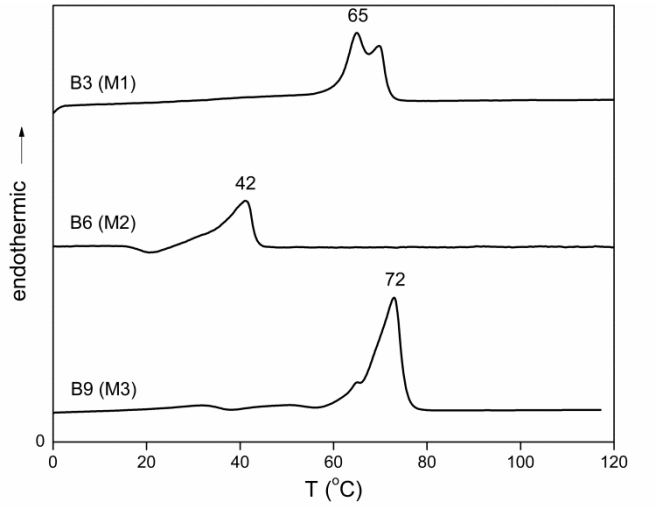

Since the goal of this study is to obtain polymeric nanoparticles by thiol-ene polymerizations in miniemulsion, the three different diene monomers (M1, M2, and M3) were used in copolymerization reactions with 1,4-butanedithiol in miniemulsion. All reactions were carried out at the same conditions of temperature (80 ºC), time (3 hours), type and amount of surfactant (SDS, 0.019 mol% related to the water) and dithiol content (1:1 dithiol-to-diene ratio) used. Table 4 shows the intensity average particle size (Dp), number average (Mn) and weight average (Mw) molecular weight of the final samples of the reactions varying the type of diene monomer and initiator (AIBN) amount.

Table 4. Formulation and results of thiol-ene polymerization reactions in miniemulsion using different α,ω-diene monomers, 1,4-butanedithiol and SDS as surfactant. Monomer type, AIBN concentration, average particles diameter (Dp) number average molecular weight (M_n) and weight average molecular weight (M_w).

Entry	Diene monomer	[AIBN] (mol%)	Dp (nm)[a]	M_n (kDa)[b]	M_w (kDa)[b]
Mini1	M2	0.25	241	6.6	10.6
Mini2	M2	0.5	290	6.0	12.8
Mini3	M2	1.0	215	5.8	13.7
Mini4	M3	0.25	132	6.3	22.0
Mini5	M3	0.5	114	10.6	25.4
Mini6	M3	1.0	138	15.3	33.9
Mini7	M3	1.5	131	8.1	18.5

[a] average particle diameter obtained by DLS; [b] GPC was performed in THF with PMMA calibration.

Reactions using 1,7-octadiene (M1) as monomer presented no stability due to its higher hydrophilicity, therefore new attempts adding a costabilizer (hexadecane or Crodamol®) to the formulation were performed and stable latexes were obtained (see Attachments). These results are not shown herein because we only wanted to compare results with the same formulation (without costabilizer).

When M2 or M3 were employed, reactions resulted in particle sizes in the range of 114-290 nm, depending on the monomer used, and polydispersity index (PdI) around 0.2. Reactions using 1,3-propylene dipent-4-enoate (M2) presented larger average particle diameters due to its higher hydrophilicity (shorter carbon chain) compared to M3.

Again, thiol-ene polymerization with M3 presented an increase in molecular weight with the increase of initiator concentration (Figure 26), achieving its maximum M_n at the concentration of 1 mol% of AIBN (Mini 6) and turning to decrease when the amount of AIBN was further increased to 1.5 mol% (Mini7).

Figure 26. GPC traces of poly(thioether-ester) samples obtained using monomer M3 under different concentrations of AIBN in miniemulsion.

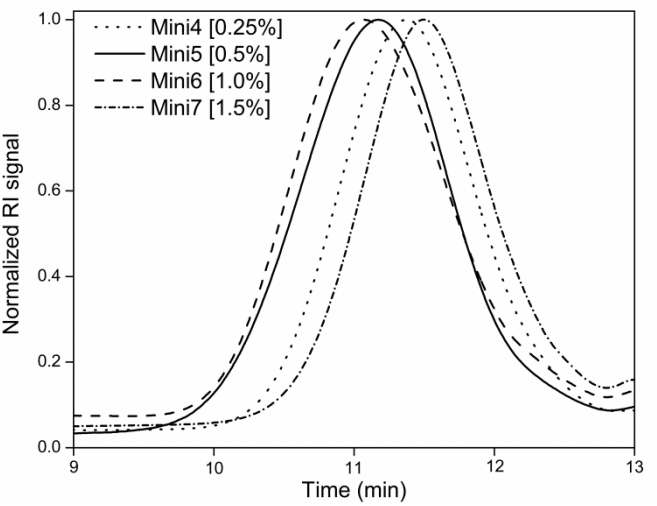

Continuing the investigation, polymerization reactions of the fully renewable monomer M3 were carried out under new conditions, such as different types of surfactant (SDS or Lutensol AT80) and dithiol (1,4-butanedithiol and 2-mercaptoethyl ether), to evaluate the effect on molecular weight distribution. The experiments in miniemulsion (shown in Table 5) resulted in particle sizes in the range of 114 –173 nm and polydispersity index (PdI) below 0.2, depending on the surfactant employed.

When comparing reactions using M3, BDT and 1 mol% of AIBN in bulk (B9) and miniemulsion (Mini6), it can be noticed similar results for molecular weight (M_w = 33 kDa), evidencing that thiol-ene reactions in miniemulsion yielded comparable results to those in bulk. However, reaction Mini8, using Lutensol AT80, presented lower molecular weight than reaction Mini6, using SDS; this result is probably due to the higher average particles diameter (Dp) obtained using Lutensol as surfactant (173 nm), since an increase in the droplet size may increase bimolecular termination probability due to the higher content of radicals inside the droplet. In miniemulsion systems, radical compartmentalization allows faster polymerization rates and higher molecular weights (LANDFESTER, 2003; COSTA *et al.*, 2013); however, thiol-ene reactions not just depend on average number of radicals per particle but mostly on the stoichiometry (CRAMER *et al.*, 2003). Therefore, radical

compartmentalization effect occurs only if the stoichiometric balance is not impaired in the polymerization locus (MACHADO *et al.*, 2016).

Table 5. Formulation and results of thiol-ene polymerization reactions using M3 and 1 mol% of AIBN. Process conditions (bulk or miniemulsion), dithiol type, surfactant type, average particles diameter (Dp), number average molecular weight (M_n) and weight average molecular weight (M_w).

Entry	Process	Dithiol	Surf.	Dp (nm)[a]	M_n (kDa)[b]	M_w (kDa)[b]
B9	Bulk	BDT	-	-	17.6	33.4
Mini6	Mini	BDT	SDS	138	15.3	33.9
Mini8	Mini	BDT	Lutensol	173	8.7	27.0
Mini9	Mini	MEE	SDS	143	5.4	18.4

[a] average particle diameter obtained by DLS; [b] GPC was performed in THF with PMMA calibration.

Also, polymer obtained with MEE in miniemulsion (Mini9), presented lower molecular weight by comparison to the polymer obtained with BDT in miniemulsion (Mini6), probably due to the high hydrophilicity of MEE (its water solubility is approximately 10 times higher than that of 1,4-butanedithiol), resulting in less thiyl radicals per nanodroplet and therefore creating a stoichiometric disbalance in the polymerization locus. As mentioned before, thiol-ene polymerization is sensitive to variations in stoichiometry and thus molecular weight is not allowed to further increase. Figure 27 shows GPC results of the poly(thioether-ester)s obtained in reactions with M3 under different conditions (B9, Mini8, Mini9).

FTIR spectra of a dried sample from reaction Mini6 is presented in Figure 28. It can be noticed that there is no peak correspondent to double bonds at 1640 cm^{-1} (C=C stretch), indicating absence of residual diene monomer. Additionally, the presence of C—S—C stretching vibration can be observed at ~710 cm^{-1}, evidencing the addition of thiyl radicals across the double bonds of the diene.

Figure 27. GPC traces of poly(thioether-ester) samples obtained using M3 and 1mol% of AIBN using different dithiols (BDT and MEE).

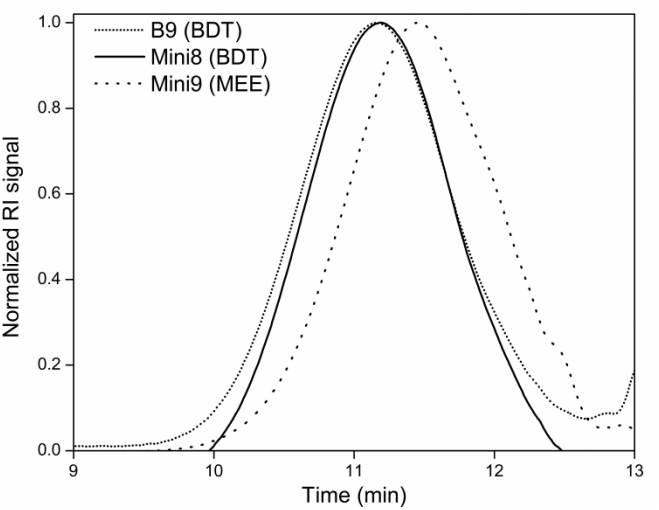

Figure 28. FTIR spectrum of a dried sample from reaction Mini6.

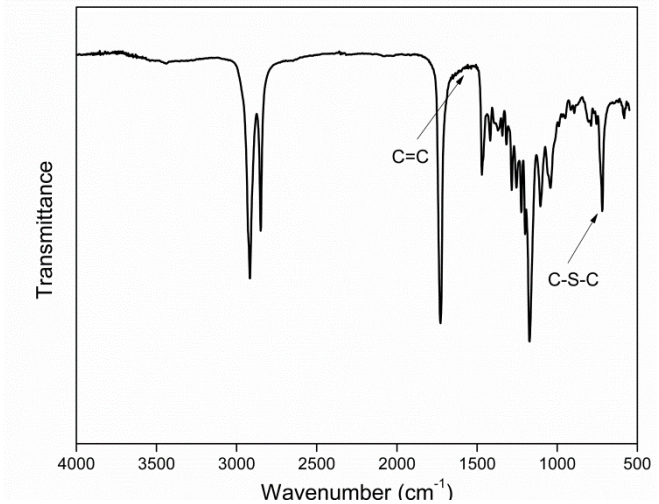

TEM images (Figure 29) of the poly(thioether-ester) latex synthesized with the fully renewable monomer M3 and BDT (Mini6) confirmed that particles with spherical morphology were obtained. It is important to mention that the morphology of non-cross-linked polymer particles with low glass transition temperature is not very often

successfully analyzed by TEM, except when cryo-TEM is available. Therefore, the TEM equipment was operated at the lowest current possible; when the current was increased during the microscopic analyses, the polymeric particles melted (T_m < 80 ºC). Figure 29 shows the particles before (a, c) and after melting (b, d).

Figure 29. Poly(thioether-ester) nanoparticles obtained by thiol-ene reaction in miniemulsion using 1 mol% of AIBN and stabilized with SDS (Mini6). Polymer particles before (a, c) and after (b, d) melting under electron beam.

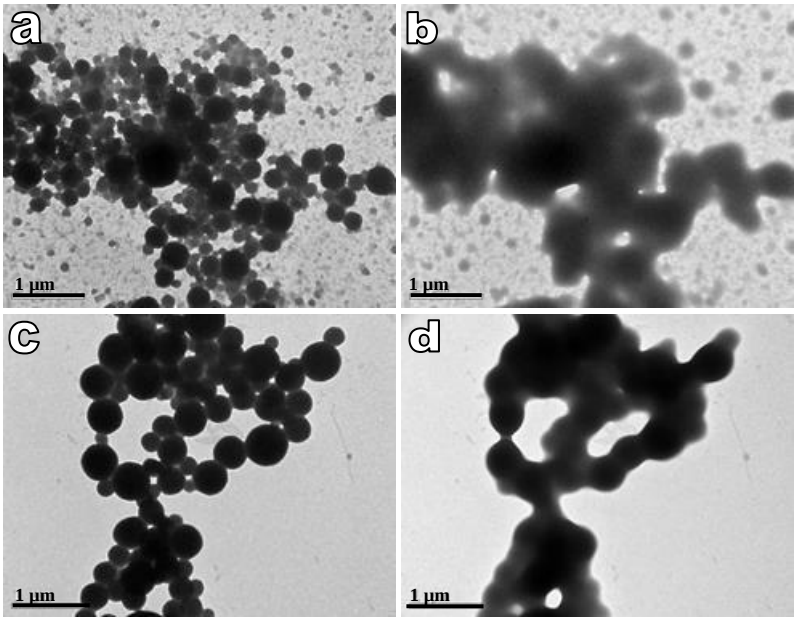

4.4 CONCLUSION

Herein, thiol-ene polymerization reactions were successfully performed in miniemulsion and poly(thioether-ester) nanoparticles were obtained from a fully renewable diene monomer derived from castor oil (1,3-propylene diundec-10-enoate). Three different α,ω-diene monomers (1,7-octadiene, 1,3-propylene dipent-1-enoate and 1,3-propylene diundec-10-enoate) and two different dithiols (1,4-butanedithiol and 2-mercaptoethyl ether) were evaluated and the results were compared. Reactions yielded polymers with weight average molecular weight up to 15.3 kDa (M_n), depending on the comonomers employed and the

initiator concentration. Additionally, AIBN (initiator) presented an ideal concentration (1 mol %) to achieve higher molecular weight, a different behavior of the observed in traditional free radical polymerization. Moreover, the synthesized poly(thioether-ester) nanoparticles derived from renewable resources present potential degradability properties (hydrolysable bonds in the main chain) and biocompatibility; therefore, the (bio)degradation of these particles and cytotoxicity/biocompatibility tests should be performed for future biomedical applications.

CHAPTER V

5 OXIDATION OF POLY(THIOETHER) TO POLYSULFONE NANOPARTICLES

This chapter is part of a publication entitled "**Oxidation of Poly(thioether) to Polysulfone Nanoparticles**", under submission.

5.1 INTRODUCTION

Thiol-ene "click" reactions can be effectively used in a large number of applications, ranging from synthetic processes for basic chemical synthesis to the fabrication of a wide range of polymeric materials and new applications, including optical displays, nano-imprinting, holographic diffractive materials, microfluidic devices, high-impact energy-absorbing devices, complex surface patterns, optical switching arrays, and functionalized linear polymers. However, applications requiring materials with high glass transition temperature (T_g), such as dental restoratives, optical components and automotive/ aerospace repair resins, are not readily achievable using most traditional thiol–ene combinations, since thioether-linkages are characterized by flexible sulfide bonds (LI, 2007; CARIOSCIA *et al.*, 2007; HOYLE; BOWMAN, 2010).

Therefore, easy post polymerization modification of polymer backbones appears as an important and challenging concept in polymer science. Hydrophobic thioether can be oxidized to more polar sulfoxide or sulfone derivatives (POTAPOV *et al.*, 2011). The presence of polar sulfone groups in polymer backbones generates interesting properties due to the strong interactions between sulfone groups (dipole moment of 4.5 Da). The high polarity of these functional groups tends to increase the T_g and thermal stability of the material, leading to a modified polymer surface energy with improved adhesion characteristics, paintability or pigment wetting (VAN DEN BERG *et al.*, 2013). Furthermore, sulfone groups present in polymer chains can also lead to liquid crystallinity (ZHANG 1994).

Because of the very low dipole moment of thioethers, these compounds are generally hydrophobic; upon oxidation, they are converted to high-dipole-moment sulfoxides and/or sulfones, leading to an increase in affinity towards water (VO; KILCHER; TIRELLI, 2009). Therefore, oxidation could act as a trigger that converts a material from hydrophobic to hydrophilic. Thus, due to the associated morphological

transitions promoted, such as the swelling of a polymer network or the solubilization of individual macromolecules, poly(sulfone) nanoparticles dispersed in a hydrophilic solvent could be used for releasing encapsulated bioactive compounds or for uncovering groups capable of specific interactions with cells (JASINSKI *et al.*, 2016).

So far, Rehor, Tirelli and Hubbell (2002, 2005) studied the synthesis of oxidation responsive poly(thioether) nanoparticles through emulsion ring-opening polymerization of propylene sulfide. Recently, Jasinski and coworkers (2016) reported the synthesis and application of poly(thioether-ester) latexes via thiol-ene miniemulsion photopolymerization. The combination of thioether and ester bonds in the same polymer backbone could provide nanoparticles potentially sensitive to oxidation and hydrolysis, acting as dual-stimuli-responsive nanocarriers (JASINSKI *et al.*, 2016).

Among the different oxidants and catalysts useful for the oxidation of thioethers, hydrogen peroxide is known as the most versatile and environmentally friendly. Furthermore, the oxidation of sensitive sulfides by hydrogen peroxide usually proceeds under relatively mild conditions and, in several cases, only a small excess of H_2O_2 is required (NOYORI; AOKI; SATO, 2003; POTAPOV *et al.*, 2011). In addition, due to its solubility in water, hydrogen peroxide is very suitable for oxidizing poly(thioether) particles dispersed in aqueous media (JEANMAIRE *et al*., 2014).

Herein, it is presented the post polymerization oxidation of poly(thioether-ester) nanoparticles, synthesized in Chapter IV, using a hydrogen peroxide solution, a well-known process to oxidize the sulfur atom successively to sulfoxide and sulfones. Morphology and thermal properties of the oxidized polymers were analyzed and compared to the original polymers (before oxidation). Furthermore, FTIR spectra of the samples were evaluated to verify the structure of the obtained materials.

5.2 EXPERIMENTAL PROCEDURE

5.2.1 Materials

Polymeric samples from reaction Mini6, obtained previously in Chapter IV. Hydrogen peroxide solution (35 wt.%, Sigma-Aldrich), sodium dodecyl sulfate (SDS, Sigma-Aldrich, 99%) and sodium bicarbonate (Vetec, 99,7%). All materials were used as received. Distilled water was used in all experiments.

5.2.2 Oxidation procedure

For solid polymer samples (previously precipitated in methanol), 0.2 g of polymer was dissolved in chloroform (20 mL) and, subsequently, hydrogen peroxide solution (35 wt.%, 0.6 mL) was added to the reaction flask (**S-OXI**).

For latex samples, 2 g of miniemulsion (0.2 g of polymer, approximately) was mixed with 6g of a SDS solution (0.25 wt.% in water) and then 0.6 mL of hydrogen peroxide solution (35 wt.%) was added dropwise (**L-OXI**).

After 3 h of reaction at 64 °C, the formed polymer was precipitated in a methanol–water (60:40) mixture. The precipitated polymer was then washed successively with sodium bicarbonate (100 mL), water (100 mL), and methanol (100 mL) prior to drying in a vacuum oven at room temperature. The procedure adopted was found in the literature (VAN DEN BERG *et al.*, 2013).

5.2.3 Particle Size Measurements

Intensity average diameters of the polymer particles (Dp) and the polydispersity indexes (PdI) were measured by dynamic light scattering (DLS - Malvern Instruments, Zeta SizerNano S). The latex samples were diluted approximately 1:15 with distilled water prior to DLS analysis.

5.2.4 Differential scanning calorimetry

DSC experiments were carried out under a nitrogen atmosphere (30 mL min-1) at a heating rate of 10 °C min^{-1} on a Mettler Toledo DSC 823 calorimeter. The melting temperature, T_m, was recorded from the second heating ramp, from -50 ºC to 180 ºC.

5.2.5 Fourier Transform Infrared Spectroscopy (FTIR)

Attenuated Total Reflectance Fourier Transform Infrared (ATR-FTIR) spectroscopy was performed on a Shimadzu spectrometer, model IRprestiage-21, in the range of wavenumbers 4000-400 cm^{-1} by accumulating 32 scans at a resolution of 4 cm^{-1}. The polymer samples were analyzed as mulls, prepared by mixing the polymer with dry KBr powder and pressing into a transparent KBr pellet.

5.2.6 Thermogravimetric Analyses (TGA)

Thermal decomposition was studied by thermogravimetric analysis (TGA, STA 449 F3 Jupiter, NETZSCH). Approximately 10 mg of each sample was weighed in a platinum pan and heated from 50 ºC to 800°C, at a heating rate of 5 ºC min^{-1}, under a nitrogen flow rate of 20 mL/min.

5.2.7 Transmission Electron Microscopy (TEM)

Particle morphology characterization was performed by Transmission Electron Microscopy using a JEM-1011 TEM (100 kV). For this analysis, the sample was diluted in distilled water down to 0.01% of solids content and one single drop was placed on a carbon-coated copper grid. Then the grid was dried under room conditions overnight. These analyses were performed in the Laboratório Central de Microscopia Eletrônica (LCME), Federal University of Santa Catarina.

5.3 RESULTS AND DISCUSSION

Aiming to modify the backbone of the polythioether samples synthesized in Chapter IV and thus obtain materials with different properties, the thioether-linkages of the polymer chains were oxidized to sulfones and sulfoxide linkages, using hydrogen peroxide solution. In the process, 4 eq. of hydrogen peroxide (in relation to the sulfur function in the polymer chain) was used. In order to compare the oxidation processes for the nanoparticles and for the polymers obtained in bulk, one aliquot of the latex obtained from reaction Mini6 (M_n=15.3 kDa; Chapter IV) was precipitated in cold methanol, the polymer was solubilized in chloroform and oxidized in solution (S-OXI), while other aliquot was oxidized in latex (aqueous miniemulsion) form (L-OXI), i.e. without polymer precipitation. After 3 hours of reaction, the resultant materials were precipitated in methanol and purified prior to characterization analyses. One aliquot of the latex material (L-OXI) was reserved for DLS and TEM measurements.

DLS measurements assured the stability of the latex after oxidation, showing that the particles size remained at 140 nm (PDI = 0.13). Figure 30 displays the Particle Size Distribution (PSD) for the nanoparticles before (Mini6) and after (L-OXI) oxidation. Also, Figure 31 shows TEM images of the oxidized latex (L-OXI) confirming

that the morphology of the nanoparticles was maintained even after the oxidation process.

Figure 30. PSD for the nanoparticles before (Mini6) and after (L-OXI) oxidation.

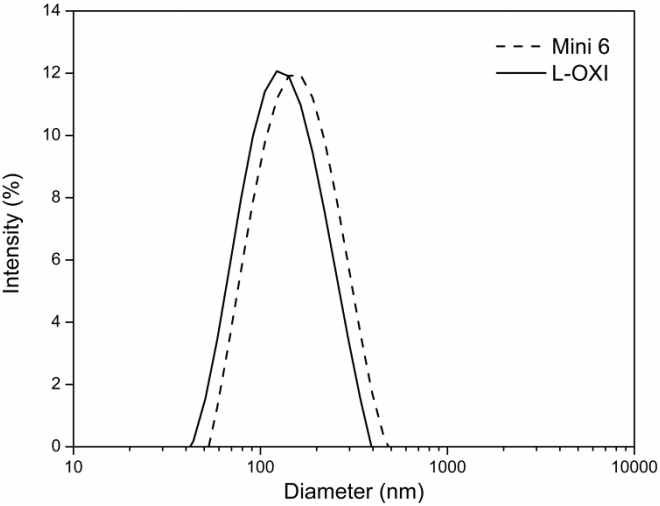

Figure 31. Polymeric nanoparticles obtained by thiol-ene reaction in miniemulsion and modified by post polymerization oxidation (L-OXI) with hydrogen peroxide.

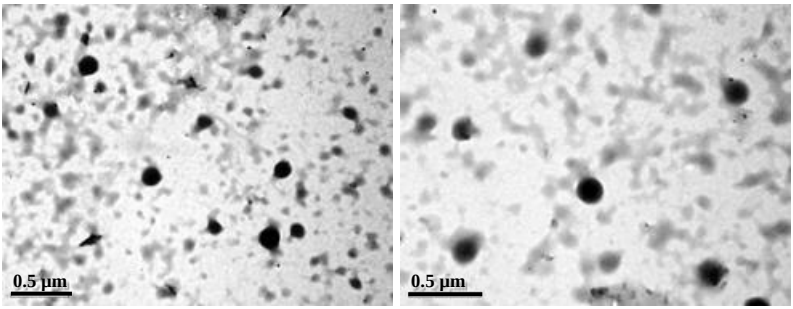

FTIR analyses (Figure 32) revealed the success of the oxidation reactions, which was confirmed by the peaks observed in 1022 cm^{-1} (sulfoxide specific IR absorption), 1126 cm^{-1} and 1257 cm^{-1} (sulfone specific IR absorptions) and 610 cm^{-1} (SO_2 scissoring).

Figure 32. FTIR spectra of the polythioether Mini6 and its oxidized forms (L-OXI and S-OXI).

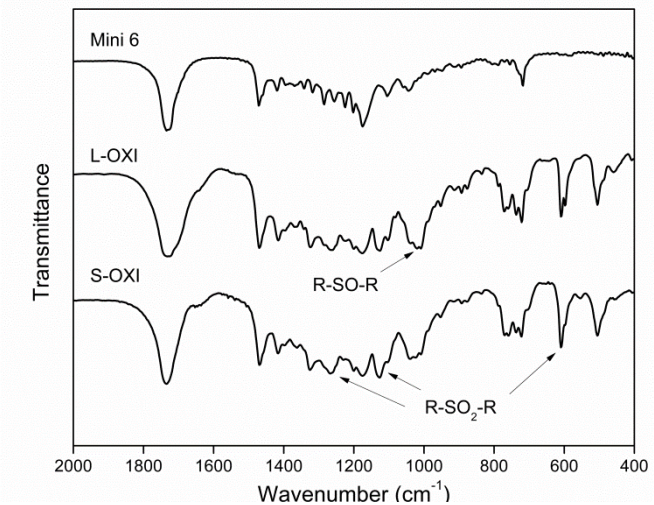

The thermal behaviors of the polymeric samples before (Mini 6) and after oxidation (L-OXI and S-OXI) were examined by thermogravimetric analyses (Figure 33). It can be noticed a thermal instability around 250 ºC for the oxidized polymers, which did not happen with the non-oxidized polymer (Mini 6). This behavior probably occurred due to the cracking of the sulfoxide groups to sulfenic acid and alkene (LEE; LITT; ROGERS, 1998). Thus, in order to further verify the degradation of the oxidized polymers, sample L-OXI was submitted to thermal decomposition up to 250 ºC (for 30 min, under nitrogen flow) and the product was analyzed by FTIR (Figure 34). The thermal instability at 250 ºC of the sulfoxide groups was confirmed by the reduction of the peak observed in 1022 cm^{-1} (sulfoxide specific IR absorption) and the intensification of the peaks in 3450 cm^{-1} (O-H stretch; indicating the sulfenic acid formation) and 1640 cm^{-1} (C=C stretch; evidencing the alkene formation).

Figure 33. TGA traces of polythioether (Mini6) and oxidized polymers (L-OXI and S-OXI).

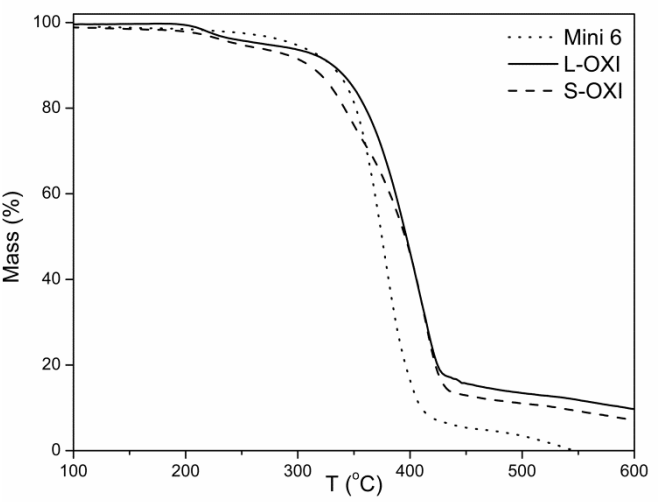

Figure 34. FTIR spectra of the oxidized polymer L-OXI and its form after thermal decomposition up to 250 ºC (L-OXI-250).

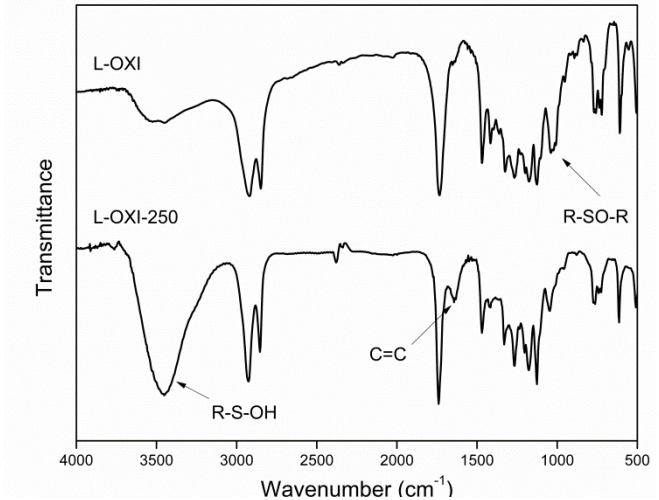

The oxidation process resulted in a significant increase of the polymers melting temperature (T_m) from 73 ºC to around 132 °C (Figure 35). Both methods, oxidation in solution (S-OXI) or latex (L-OXI), presented similar results, corroborating the success of the oxidation

process for the nanoparticles in aqueous miniemulsion. In addition, it can be noticed that oxidized polymers presented broader peaks in comparison to the sample before oxidation; such behavior is attributed for the recrystallization of different crystal forms in polar polymeric materials (VAN DEN BERG *et al.*, 2013).

Figure 35. DSC traces of poly(thioether) samples without oxidation (Mini6) and oxidized in solid form (S-OXI) and latex (L-OXI).

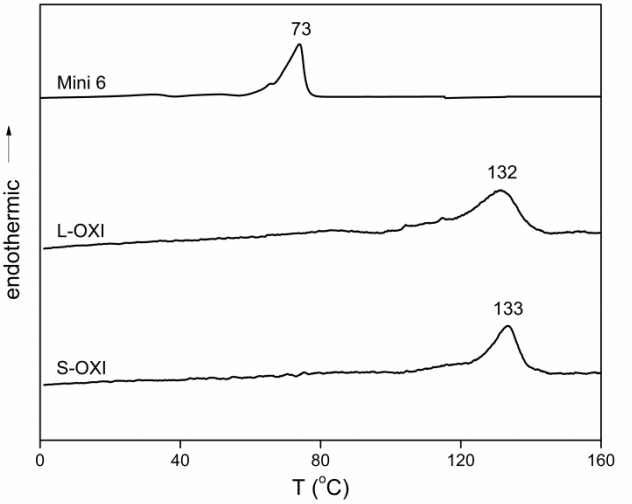

As expected, all the oxidized polymeric samples were no longer soluble in any solvent tested, including THF; therefore, it was not possible to determine their molecular weights by GPC. Moreover, other analyses, such as tensile testing and AFM (Atomic Force Microscopy), must be performed in future works for further characterization of the obtained polymers and biocompatibility and cytotoxicity tests of the modified nanoparticles should be evaluated for future biomedical applications.

5.4 CONCLUSION

Herein, poly(thioether-ester) nanoparticles, previously obtained through thiol-ene reactions in miniemulsion, were modified by post-polymerization oxidation of the thioether groups. A well-established process to oxidize the sulfur atom was performed using a hydrogen peroxide solution. For comparison of the results, the polymeric samples

were submitted to oxidation in latex and solution forms. FTIR measurements assured the appearance of sulfoxide and sulfone groups after the oxidation and TGA-analyses showed a thermal instability around 250 ºC, which was attributed to the sulfoxide groups and confirmed by FTIR. The melting temperature (T_m) of the oxidized polymers increased to 132 ºC and broader melting peaks were observed, probably due to the recrystallization of different crystals in polar polymeric materials. In addition, the size/dispersion stability and morphology of the nanoparticles after oxidation was confirmed by DLS and TEM images. Lastly, oxidized nanoparticles obtained herein present high potential for the release of bioactive compounds and, therefore, biocompatibility/cytotoxicity analyses should be performed for future biomedical applications.

CHAPTER VI

6 CITOTOXICITY AND BIOCOMPATIBILITY OF THE POLY(THIOETHER-ESTER) NANOPARTICLES

6.1 INTRODUCTION

Polymeric nanoparticles have been earning significant attention as drug carriers due to many advantages, such as protective effect against drug degradation, controlled or sustained release, possibility of drug delivery within the target tissue, and reduction of side effects (DE JONG; BORM, 2008; FELICE *et al*., 2014; FEUSER *et al*., 2016). In this field, miniemulsion polymerization allows the synthesis of polymeric NPs with unique characteristics and great commercial interest, with the possibility of using and/or incorporating drugs with low solubility in the continuous phase for a wide range of applications. Furthermore, miniemulsion polymerization is a versatile technique and presents some attractive advantages such as easier temperature control and radical compartmentalization inside the polymer particles (promoting high polymerization rates and allowing to obtain high molecular weight polymers) (EL-AASSER; MILLER, 1997; ASUA, 2002; ANTONIETTI; LANDFESTER, 2002; SCHORK *et al.*, 2005; CARDOSO; ARAUJO; SAYER, 2013).

In this context, biobased polymers obtained from vegetable oils present potential biodegradability and biocompatibility, allowing their application for biomedical purposes. Thiol-ene reactions appear as successful and versatile techniques to obtain high molecular weight polymers from renewable raw materials, affording products with improved mechanical properties, unique crosslinking structure and tunable degradability behavior (KADE; BURKE; HAWKER, 2010; HOYLE; LOWE; BOWMAN, 2010). In addition, thiol-ene reactions allow the synthesis of polyesters in aqueous dispersed medium and thereby are suitable for the production of polymeric nanoparticles containing ester groups in the main chain, which can undergo hydrolysis, allowing their degradation in physiological environment, which is of great importance for biomedical applications or material disposal (JASINSKI *et al.*, 2014). However, little attention has been paid to the synthesis of biocompatible and biodegradable polymers through thiol-ene polymerization. Studies regarding the use of thiol-ene based polymeric nanoparticles in the biomedical field, portraying

biocompatibility and biodegradation, are still underexplored (ZOU *et al*., 2011; MACHADO; SAYER; ARAÚJO, 2016).

Thereby, the goal of this study was to characterize the biobased poly(thioether-ester) nanoparticles synthesized in Chapter IV, focusing on future biomedical applications. Biocompatibility assays were performed in murine fibroblast (L929) cells and human cervical cancer cells (HeLa). Morphological analyses of the cells were carried out by inverted microscopy. Additionally, the effect of the nanoparticles in normal red blood cells (RBC) was verified by hemolysis assay.

6.2 EXPERIMENTAL PROCEDURE

6.2.1 Biocompatibility assay on L929 (murine fibroblast) cells

The L929 cell lines were selected to evaluate cytotoxicity as a direct contact test, as recommended by ISO 10993 for *in vitro* toxicity. The cells were cultured in Dulbecco's Modified Eagle's medium (DMEM) supplemented with 10% fetal bovine serum, penicillin (100 units/ml), streptomycin (100 mg/mL), and 4 mM/L of glutamine at 37 °C in tissue culture flasks with 5 % CO_2. For experimental purposes, trypsinized cells were adjusted to a concentration of $1x10^4$ cells plated in a 96-well flat bottom culture plate. For the cytotoxicity study, the cells were incubated for 24 h (5% CO_2, 37 °C) in five different concentrations (25, 50, 75, 100 and 200 µg/mL) of the polymeric nanoparticles (PTEE-N) dispersed in PBS 7.4. After 24 h of incubation the nanoparticles were washed three times with PBS (phosphate buffered saline) and cell viability was assessed using the classical MTT assay (Sigma, MO, USA).

6.2.2 Cytotoxicity assay on HeLa (human cervical cancer cells)

HeLa cell lines were obtained from the Adolfo Lutz Institute (São Paulo). HeLa cells were grown in Minimum Essential Medium (MEM) containing 7.5% fetal bovine serum and maintained at 37 °C in a humidified incubator containing 5% CO_2. The HeLa cells were seeded at $1x10^4$ cells/well in a 96-well flat bottom culture plate. After 24 h, the cells were incubated with a medium containing polymeric nanoparticles (PTEE-N) dispersed in PBS 7.4 at five concentrations: 25, 50, 75, 100 and 200 µg/mL (5% CO_2, 37 °C). After 24 h of incubation the cells were washed three times with PBS (7.4) and the MTT cell viability assay was

performed. The cytotoxicity assay was carried out in triplicate, with three wells for each condition.

6.2.3 MTT viability assay

The MTT cell proliferation assay was employed to assess cell viability after both cytotoxic assays. Briefly, 200 µL aliquots of MTT solution (5 $mg.mL^{-1}$) were added to each well and incubated for 3 h (37 °C and 5% CO_2), to allow the formazan-formation reaction. Following incubation, the medium containing the MTT solution was removed and the formazan crystals were dissolved in DMSO. The absorbance was measured at 550 nm using an Infinite 200 TECAN microplate reader. The results are presented as survival percentage (100%), where the control group contained 1% DMSO (v/v).

6.2.4 Morphological analyses

Morphological analyses, consistent with observation of changes in cells morphology, were carried out by inverted microscopy (40X). Cells were incubated with poly(thioether-ester) nanoparticles (PTEE-N) at the concentration of 50 µg/mL. As negative controls, cells were analyzed without incubation (control group). The morphological changes of the cells were observed 24 h after the incubation.

6.2.5 Hemolysis Assay

In order to analyze the effect of nanoparticles in normal red blood cells (RBC), five human blood samples were collected according to the ethics committee requirements (CEPSH n° 913/2010). Briefly, 4 mL of whole blood was added to 8 mL of a sterile solution of sodium chloride in water (saline) and the RBCs were isolated from serum by centrifugation at 10,000 × *g* for 5 min. The RBCs were further washed five times with saline solution, after that, the RBCs were diluted in 2 mL of saline solution. Then 120 µL of the diluted RBC suspension was added to 880 µL of water or saline. Samples were incubated with polysulfone nanoparticles (PS-N) at a concentration of 50, 100 and 200 µg/mL. All samples were prepared in triplicate and the suspension was briefly vortexed before undergoing a gentle stirring at 37 °C for 60 min. Afterwards, the mixture was briefly vortexed again and centrifuged at 10.000 × *g* for 5 min. 100 µL of supernatant was transferred to a 96-well plate. The absorbance value of hemoglobin at

570 nm was measured with the reference wavelength at 540 nm. 120 µL of the diluted RBC suspension incubated with 880 µL of water and saline were used as the positive and negative control, respectively (WANG *et al.*, 2009; YU; MALUGIN; GHANDEHARI; 2011). Hemolysis percentage was calculated according to Eq. 1:

$$Hemolysis\ (\%) = \frac{\text{Sample absorbance} - \text{negative control}}{\text{positive control} - \text{negative control}}\ x\ 100 \qquad \text{Eq. (1)}$$

6.2.6 Statistical analysis

Data are presented as the mean ± standard deviation of three determinations. One-way ANOVA followed by the Bonferroni *post hoc* test were used to compare the cytotoxicity of the samples at different concentrations. Statistical analysis was performed using the Statistical Package for Social Sciences for Windows (SPSS Inc. version 13.0, USA). The statistical significance level was set at $p < 0.05$ for all analyses.

6.3 RESULTS AND DISCUSSION

Cytotoxic effects of the synthesized poly(thioether-ester) nanoparticles (**PTEE-N**; Mini6 from Chapter IV) were evaluated by MTT assay on HeLa and L929 cells. Figure 36 and Figure 37 show the cytotoxicity profiles of HeLa and L929 cells, respectively, incubated with different concentrations of PTEE-N nanoparticles. It could be observed that the nanoparticles did not present any cytotoxic effect.

Figure 36. Cytotoxicity effects of different concentrations of PTEE-N nanoparticles on HeLa cells, after 24 hours of incubation. ($p < 0.05$ compared to control group, using ANOVA followed by the Bonferroni *post hoc* test).

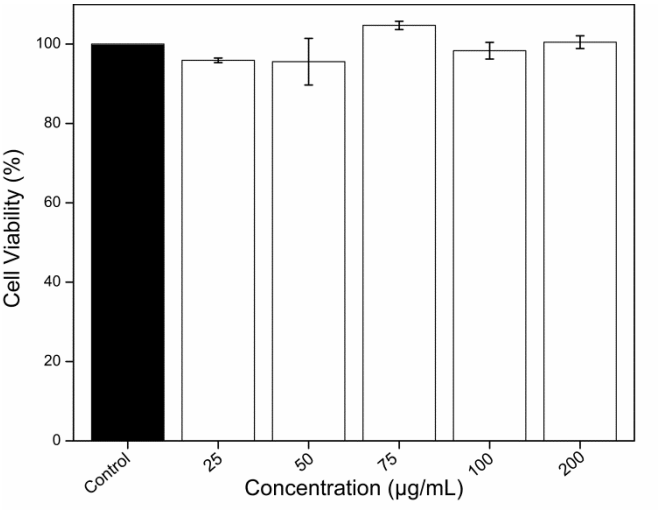

Figure 37. Cytotoxicity effects of different concentrations of PTEE-N nanoparticles on L929 cells, after 24 hours of incubation. ($p < 0.05$ compared to control group, using ANOVA followed by the Bonferroni *post hoc* test).

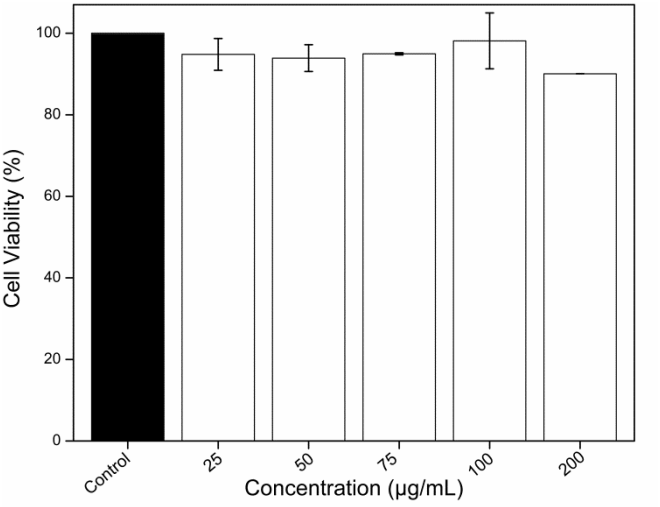

Additionally, Figure 38 shows that there were no significant changes in cell morphology after the incubation with PTEE-N nanoparticles on HeLa (a) and L929 (b) cells. The non-cytotoxicity of the L929 cells is an important factor; ISO 10993-5 recommends in vitro cytotoxicity assay of new materials for biomedical application. According to ISO 10993-5, cell viability < 70% compared to untreated cells are considered cytotoxic (MADERUELO; ZARZUELO; LANAO, 2011). Therefore, after the observed results, it can be said that poly(thioether-ester) nanoparticles obtained in this work are biocompatibles.

Figure 38. Morphology of HeLa and L929 cells incubated with 50 µg.mL^{-1} of PTEE-N nanoparticles for 24 hours. HeLa (a) and L929 (c) control cells; HeLa (b) and L929 (d) cells after incubation. (Magnification 40X).

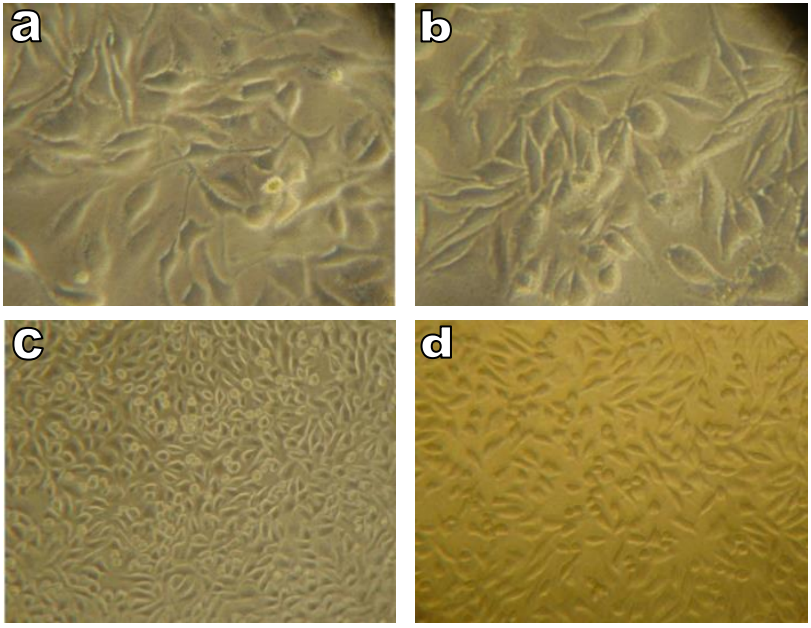

Moreover, the impact of the poly(thioether-ester) nanoparticles (PTEE-N) on human red blood cells (RBCs) was evaluated by hemolysis assay (Figure 39). The quantification of hemoglobin in the supernatant of the nanoparticle-RBC mixture was done by recording the absorbance of hemoglobin at 540 nm. Treatments with 50 µg/L, 100 µg/L and 200 µg/L were not able to cause hemolysis of RBCs,

suggesting that these systems do not have hemolytic capacity, even when administered at high concentrations. These results reveal that PTEE-N nanoparticles have high blood biocompatibility, making them a potential alternative to carry drugs intravenously.

Figure 39. Hemolysis assay. Relative rate of hemolysis in human RBCs upon incubation with PS-N nanoparticles at 50 µg/L, 100 µg/L and 200 µg/L for 24 hours. The presence of hemoglobin in the supernatant (red) was observed at 540 nm. Data are mean ± SD (n = 3).

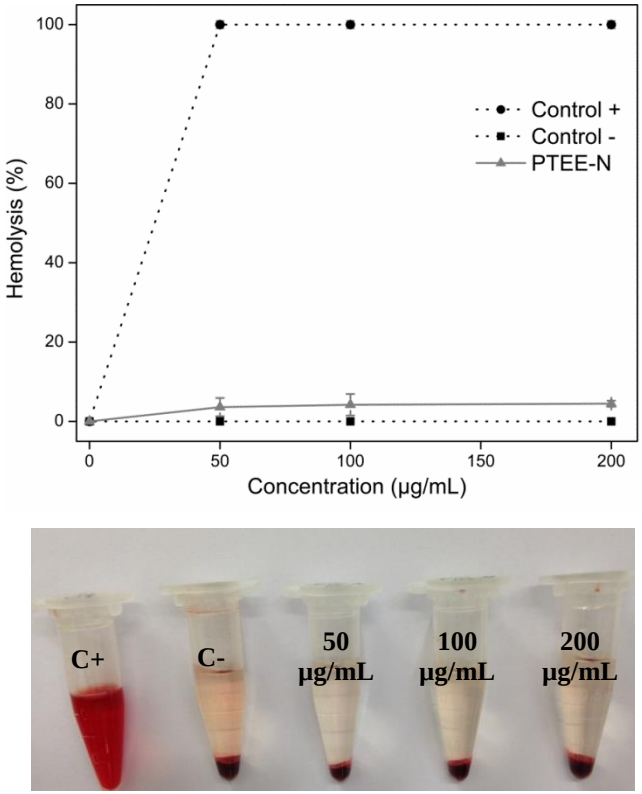

6.4 CONCLUSION

This work has demonstrated that the synthesized poly(thioether-ester) nanoparticles (PTEE-N) derived from renewable resources did not present any cytotoxic effect in murine fibroblast cells (L929) and human

cervical cancer cells (HeLa). Also, it was observed no significant changes in cell morphology after the incubation with PTEE-N on HeLa and L929 cells, confirming the biocompatibility of the poly(thioether-ester) nanoparticles and assuring their viability for biomedical purposes. In addition, hemolysis assays revealed that PTEE-N nanoparticles have high blood biocompatibility, making them a potential alternative as drug carrier systems for intravenous applications.

CHAPTER VII

7 FINAL CONSIDERATIONS

7.1 CONCLUSION

In this work, the synthesis and characterization of a 100% renewable diene-diester monomer derived from 10-undecenoic acid (a castor oil derivative) and 1,3-propanediol (derived from glycerol) was reported. This green monomer was submitted to ADMET and thiol-ene polymerization reactions in miniemulsion aiming the development of biobased polymeric nanoparticles.

ADMET reactions were successfully performed in miniemulsion and the obtained polymers achieved weight average molecular weight up to 14.7 kDa (M_n), depending on the catalyst and the surfactant employed. It was observed that the Ru-indenylidene catalyst (Umicore M2) presented higher activity in water by comparison to the Ru-benzylidene catalysts (Grubbs 1st and Hoveyda-Grubbs 2nd), corroborating previous results from the literature concerning the higher robustness of indenylidene catalysts. Additionally, the catalysts activity was significantly affected by the type of the surfactant, depending on its electronic charge. Moreover, ADMET reactions in miniemulsion favored the production of polymers with higher molecular weights than in bulk, probably because of the large surface area of the organic phase in miniemulsion, which causes the improvement of the ethylene removal from the reaction locus.

Also, thiol-ene polymerization reactions in miniemulsion were successfully performed and poly(thioether-ester) nanoparticles (confirmed by TEM analyses) were obtained from the fully renewable diene-diester monomer. Three different α,ω-diene monomers (1,7-octadiene, 1,3-propylene dipent-1-enoate and 1,3-propylene diundec-10-enoate) and two different dithiols (1,4-butanedithiol and 2-mercaptoethyl ether) were tested and the results were compared. Reactions yielded polymers with number average molecular weight up to 15.3 kDa (M_n), depending on the comonomers employed and the initiator concentration. Moreover, the initiator AIBN presented an ideal concentration (1 mol %) to synthesize polymers with higher molecular weight, differing from the expected behavior in traditional free radical polymerization. Furthermore, the synthesized nanoparticles from renewable raw materials present properties (such as hydrolysable bonds in the polymeric main chain) that could enhance their degradability and,

therefore, the (bio) degradation of these particles will be investigated for future applications.

Thereafter, the poly(thioether-ester) nanoparticles were modified by a post-polymerization reaction using hydrogen peroxide in order to oxidize their sulfur atom to sulfoxide and sulfone groups. DLS and TEM images assured the stability of size/dispersion and morphology of the nanoparticles even after the oxidation process. FTIR and TGA analyses confirmed the presence of sulfoxide and sulfone groups after the oxidation. The melting temperature (T_m) of the oxidized polymers increased from 73 ºC to 132 ºC and broader melting peaks were observed, attributed to the recrystallization of different crystals in polar polymers.

Finally, since the biobased polymeric nanoparticles obtained herein present high potential for the release of bioactive compounds, biocompatibility/cytotoxicity analyses were performed and results revealed that the synthesized nanoparticles did not present any cytotoxic effect and showed high blood biocompatibility, assuring their viability for biomedical purposes.

7.2 FURTHER WORK

- To synthesize other types of diene monomers from renewable resources;
- To evaluate the effect of oxygen inhibition for ADMET reactions in miniemulsion;
- To further investigate the kinetics of thiol-ene reactions, in order to explain the ideal concentration of AIBN for improved molecular weight;
- To evaluate the (bio) degradation of the obtained poly(thioether-ester) nanoparticles. Since they present ester groups in the main chain, the synthesized polymers are susceptible to hydrolysis (this work was already performed in our research group by HOELSCHER (2016));
- To finish tests concerning the biocompatibility of the synthesized nanoparticles (after oxidation) by evaluating hemocompatibility and *in vitro* cytotoxicity in fibroblast cells;
- To encapsulate bioactive compounds via thiol-ene reactions for further biomedical applications.

REFERENCES

ADEKUNLE, O.; TANNER, S.; BINDER, W. H. Synthesis and crossover reaction of TEMPO containing block copolymer via ROMP. **Beilstein Journal of Organic Chemistry**, v. 6, n. 59, 2010.

AMATO, D. V. *et al.* Functional sub-100 nm polymer nanoparticles via thiol-ene miniemulsion photopolymerization. **Polymer Chemistry**, v. 6, p. 5625–5632, 2015.

ANTONIETTI, M.; LANDFESTER, K. Polyreactions in miniemulsions. **Progress in Polymer Science**, v. 27, p. 689–757, 2002.

ASUA, J. M. Miniemulsion polymerization. **Progress in Polymer Science**, v. 27, p. 1283–1346, 2002.

AUTRAN, C.; CAL, J. C.; ASUA, J. M. (Mini)emulsion polymerization kinetics using oil-soluble initiators. **Macromolecules**, v. 40, p. 6233–6238, 2007.

BARRAULT, J.; POUILLOUX, Y. Synthesis of fatty amines. Selectivity control in presence of multifunctional catalysts. **Catalysis Today**, v. 37, p. 137–153, 1997.

BAUGHMAN, T. W.; WAGENER, K. B. Recent advances in ADMET polymerization. **Advances in Polymer Science**, v. 176, p. 1–42, 2005.

BELGACEM, M. N.; GANDINI, A. (EDS.). **Monomers , Polymers and Composites**. 1. ed. Amsterdam, Boston, Heidelberg, London, New York, Oxford, Paris, San Diego, San Francisco, Singapore, Sydney, Tokyo: Elsevier, 2008. p. 39–66.

BERNARDY, N. *et al*. Nanoencapsulation of quercetin via miniemulsion polymerization. **Journal of Biomedical Nanotechnology**, v. 6, p. 181–186, 2010.

BEYAZKILIC Z. *et al.,* Fully biobased triblock copolyesters from l-lactide and sulfur-containing castor oil derivatives: Preparation, oxidation and characterization. **Polymer**, v. 68, p. 101–110, 2015.

BIERMANN, U. *et al*. New syntheses with oils and fats as renewable raw materials for the chemical industry. **Angewandte Chemie International Edition**, v. 39, p. 2206–2224, 2000.

BIERMANN, U. *et al. O*ils and fats as renewable raw materials in chemistry. **Angewandte Chemie International Edition**, v. 50, p. 3854–3871, 2011.

BRAUN, J. V.; MURJAHN, R. Haftfestigkeit organischer Reste (IV). **European Journal of Inorganic Chemistry**, v. 59, p. 1202–1209, 1926.

BURTSCHER, D. *et al.* Controlled living ring-opening metathesis polymerization with a ruthenium indenylidene initiator. **Journal of Polymer Science Part A: Polymer Chemistry**, v. 46, p. 4630–4635, 2008.

CALDERON, N. The olefin metathesis reaction. **Accounts of Chemical Research**, v. 5, p. 127–132, 1972.

CALDERON, N.; CHEN, H. Y.; SCOTT, K. W. Olefin metathesis – A novel reaction for skeletal transformations of unsaturated hydrocarbons. **Tetrahedron Letters**, v. 34, p. 3327–3329, 1967.

CAPEK, I. On inverse miniemulsion polymerization of conventional water-soluble monomers. **Advances in Colloid and Interface Science**, v. 156, p. 35–61, 2010.

CARDOSO, P. B. *et al*. ADMET reactions in miniemulsion. **Journal of Polymer Science, Part A: Polymer Chemistry**, v. 52, p. 1300–1305, 2014.

CARDOSO, P. B.; ARAÚJO, P. H. H.; SAYER, C. Encapsulation of jojoba and andiroba oils by miniemulsion polymerization. Effect on molar mass distribution. **Macromolecular Symposia**, v. 324, p. 114–123, 2013.

CARIOSCIA, J. A. *et al.* Thiol–norbornene materials: Approaches to develop high T_g thiol–ene polymers. . **Journal of Polymer Science Part A: Polymer Chemistry**, v. 45, p. 5686–5696, 2007.

CARLSON, D. D.; KNIGHT, A. R. Reactions of thiyl radicals. XI. Further investigations of thiol-disulfide photolysis in the liquid phase. **Canadian Journal of Chemistry**, 1973.

CHOU Y.J.; EL-AASSER, M. S.; VANDERHOFF, J.W. Mechanism of emulsification of styrene using hexadecyltrimethylammonium bromide-cetyl alcohol mixtures. **Journal of Dispersion Science and Technology**, v. 1, p. 129–150, 1980.

CLAUDINO, M. Thiol–ene coupling of renewable monomers: At the forefront of bio-based polymeric materials. 2011. 63 f. Dissertação (Licentiate Thesis) - Kungliga Tekniska Högskolan, Estocolmo, 2011.

COSTA, C. *et al*. Compartmentalization effects on miniemulsion polymerization with oil-soluble initiator. **Macromolecular Reaction Engineering,** v. 7, p. 221–231, 2013.

CRAMER, N. B. *et al*. Mechanism and modeling of a thiol-ene photopolymerization. **Macromolecules**, v. 36, n. 12, p. 4631–4636, 2003.

DE JONG, W. H.; BORM, P. J. A. Drug delivery and nanoparticles: Applications and hazards. **International Journal of Nanomedicine**, v. 3, p. 133–149, 2008.

EL-AASSER, M. S.; MILLER, C. M. Preparation of latexes using miniemulsions. In: ASUA, J. M. (Ed.). **Polymeric Dispersions: Principles and Applications**. 1. ed. Dordrecht: Kluwer Academic Publishers, 1997. p. 109–126.

FELICE, B. *et al*. Drug delivery vehicles on a nano-engineering perspective. **Materials Science and Engineering: C**, v. 41, p. 178–195, 2014.

FERREIRA, V. F.; DA SILVA, F. DE C. Metátese em síntese orgânica e o prêmio nobel de química de 2005: Do plástico à indústria farmacêutica. **Química Nova na Escola**, n. 22, p. 15–20, 2005.

FEUSER *et al*., Synthesis of ZnPc loaded poly(methyl methacrylate) nanoparticles via miniemulsion polymerization for photodynamic

therapy in leukemic cells. **Materials Science and Engineering: C**, v. 60, p. 458–466, 2016.

FIRDAUS, M. *et al.* Renewable co-polymers derived from castor oil and limonene. **European Journal of Lipid Science and Technology**. v. 116, p. 31–36, 2014.

FIRDAUS, M.; MONTERO DE ESPINOSA, L.; MEIER, M. A. R. Terpene-Based Renewable Monomers and Polymers via Thiol-Ene Additions. **Macromolecules**, v. 44, p. 7253–7262, 2011.

FOCARETE, M. L. *et al.* Physical characterization of poly(ω-pentadecalactone) synthesized by lipase-catalyzed Ring-Opening Polymerization. **Journal of Polymer Science Part B: Polymer Physics**, v. 39, p. 1721–1729, 2001.

FOKOU, P. A; MEIER, M. A R. Studying and suppressing olefin isomerization side reactions during ADMET polymerizations. **Macromolecular Rapid Communications**, v. 31, p. 368–73, 2010.

FREDERICO, D.; BROCKSOM, U.; BROCKSOM, T. J. A reação de metátese de olefinas: Reorganização e ciclização de compostos orgânicos. **Química Nova**, v. 28, p. 692–702, 2005.

GANDINI, A. Polymers from renewable resources: A challenge for the future of macromolecular materials. **Macromolecules**, v. 41, p. 9491–9504, 2008.

GILBERT, R. G. **Emulsion polymerization, a mechanistic approach.** 1 ed. San Diego: Academic Press, 1995.

GRUBBS, R. H. Olefin metathesis. **Tetrahedron**, v. 60, p. 7117–7140, 2004.

GÜNER, F. S.; YAĞCI, Y.; ERCIYES, A. T. Polymers from triglyceride oils. **Progress in Polymer Science**, v. 31, p. 633–670, 2006.

HANSEN, F. K.; UGELSTAD, J.; Particle Nucleation in Emulsion Polymerization. IV. Nucleation in Monomer Droplets. **Journal of Polymer Science: Polymer Chemistry Edition**, v. 17, p. 3069–3082, 1979.

HEDMAN, B. *et al.* Synthesis and characterization of surfactants via epoxidation of tall oil fatty acid. **Journal of Surfactants and Detergents**, v. 6, p. 47–53, 2003.

HÉRISSON, J.L.; CHAUVIN, Y. Catalysis of olefin transformations by tungsten complexes. II. Telomerization of cyclic olefins in the presence of acyclic olefins. **Makromolekulare Chemie,** v. 141, p. 161–176, 1971.

HOELSCHER, F. Estudo da Degradação Hidrolítica de Filmes e Nanopartículas de Poli(tioéter-éster). 2016. 89 f. Dissertação (Mestrado) – Programa de Pós-Graduação em Engenharia Química, Universidade Federal de Santa Catarina, Florianópolis, 2016.

HOYLE, C. E. *et al*. Photoinitiated polymerization of selected thiol-ene systems. In Belfield, K. D.; Crivello, J. V., Eds.; **Photoinitiated Polymerization.** ACS Symposium Series 847; American Chemical Society: Washington, DC, 2003. p. 52–64.

HOYLE, C.E., LEE, T.Y.; ROPER, T. Thiol-enes: Chemistry of the past with promise for the future. **Journal of Polymer Science Part A: Polymer Chemistry**, v. 42, p. 5301–5338, 2004.

HOYLE, C.E.; BOWMAN, C.N. Thiol-ene click chemistry. **Angewandte Chemie International Edition**, v. 49, p. 1540–1573, 2010.

HOYLE, C.E.; LOWE, A.B.; BOWMAN, C.N. Thiol-click chemistry: a multifaceted toolbox for small molecule and polymer synthesis. **Chemical Society Reviews**, v. 39, p. 1355–1387, 2010.

IVIN, K.; MOL, J. C. **Olefin metathesis and metathesis polymerization**. 1. ed. San Diego, London: Academic Press, 1997.

JASINSKI, F. *et al.* Light-Mediated Thiol−Ene Polymerization in Miniemulsion: A Fast Route to Semicrystalline Polysulfide Nanoparticles. **ACS Macro Letters**, v. 3, p. 958–962, 2014.

JASINSKI, F. *et al.* Thiol−Ene Linear Step-Growth Photopolymerization in Miniemulsion: Fast Rates, Redox-Responsive

Particles, and Semicrystalline Films. **Macromolecules**, v. 49, p. 1143–1153, 2016.

JEANMAIRE, D. *et al*. Chemical Specificity in REDOX-Responsive Materials: The Diverse Effects of Different Reactive Oxygen Species (ROS) on Polysulfide Nanoparticles. **Polymer Chemistry**, v. 5, p. 1393−1404, 2014.

KADE, M. J.; BURKE, D. J.; HAWKER, C. J. The power of thiol-ene chemistry. **Journal of Polymer Science Part A: Polymer Chemistry**, v. 48, p. 743–750, 2010.

KARAK, N.; RANA, S.; CHO, J.W. Synthesis and characterization of castor-oil-modified hyperbranched polyurethanes. **Journal of Applied Polymer Science**, v. 112, p. 736–743, 2009.

KHARASCH, M.S.; READ, A.T.; MAYO, F.R. The peroxide effect in the addition of reagents to unsaturated compounds. XVI. The addition of thioglycolic acid to styrene and isobutylene. **Chemistry and Industry**, v. 57, p. 752, 1938.

KOLB, N.; MEIER, M. A. R. Grafting onto a renewable unsaturated polyester via thiol–ene chemistry and cross-metathesis. **European Polymer Journal**, v. 49, p. 843–852, 2013.

KREUTZER, U. R. Manufacture of fatty alcohols based on natural fats and oils. **Journal of the American Oil Chemists' Society**, v. 61, p. 343–348, 1984.

KREYE, O.; TÓTH, T.; MEIER, M. A. R. Copolymers derived from rapeseed derivatives via ADMET and thiol-ene addition. **European Polymer Journal**, v. 47, p. 1804–1816, 2011.

LANDFESTER, K. *et al.* Formulation and stability mechanisms of polymerizable miniemulsions. **Macromolecules**, v. 32, p. 5222–5228, 1999.

LANDFESTER, K. Miniemulsion polymerization and the structure of polymer and hybrid nanoparticles. **Angewandte Chemie International Edition**, v. 48, p. 4488–4507, 2009.

LANDFESTER, K. Miniemulsions for nanoparticles synthesis. **Topics in Current Chemistry**, v. 227, p. 75–123, 2003.

LANDFESTER, K. Synthesis of colloidal particles in miniemulsions. **Annual Review of Materials Research**, v. 36, p. 231–279, 2006.

LANDFESTER, K.; MUSYANOVYCH, A.; MAILÄNDER, V. From polymeric particles to multifunctional nanocapsules for biomedical applications using the miniemulsion process. **Journal of Polymer Science Part A: Polymer Chemistry**, v. 48, p. 493–515, 2010.

LEE, J. C.; LITT, M. H.; ROGERS C. E. Synthesis and Properties of Poly(oxyethylene)s Containing Thioether, Sulfoxide, or Sulfone Groups. **Journal of Polymer Science Part A: Polymer Chemistry**, v. 36, p. 793–801, 1998.

LI, Q. *et al*. Thiourethane-based thiol-ene high Tg networks: Preparation, thermal, mechanical, and physical properties **Journal of Polymer Science Part A: Polymer Chemistry**, v. 45, p. 5103–5111, 2007.

LLIGADAS, G. *et al.* Oleic and undecylenic acids as renewable feedstocks in the synthesis of polyols and polyurethanes. **Polymers**, v. 2, p. 440–453, 2010.

LLUCH, C. *et al.* Rapid approach to biobased telechelics through two one-pot thiol-ene click reactions. **Biomacromolecules**, v. 11, p. 1646–1653, 2010.

LOBRY, E. *et al*. Continuous-flow synthesis of polymer nanoparticles in a microreactor via miniemulsion photopolymerization. **RSC Advances**, v. 4, p. 43756-43759, 2014.

LOTTI, N. *et al.* Sulphur-containing polymers: Synthesis and thermal properties of novel polyesters based on dithiotriethylene glycol. **European Polymer Journal,** v. 42, p. 3374–3382, 2006.

LOWE, A. B. Thiol-ene “click” reactions and recent applications in polymer and materials synthesis. **Polymer Chemistry**, v. 1, p. 17–36, 2010.

LU, Y.; LAROCK, R. C. Novel biobased plastics, rubbers, composites, coatings and adhesives from agricultural oils and by-products. **ACS Symposium Series**, v. 1043, p. 87–102, 2010.

LYNN, D. M.; KANAOKA, S.; GRUBBS, R. H. Living ring-opening metathesis polymerization in aqueous media catalyzed by well-defined ruthenium carbene complexes. **Journal of the American Chemical Society**, v. 118, p. 784–790, 1996.

MACHADO, T. O.; SAYER, C.; ARAÚJO, P. H. H. Thiol-ene polymerisation: A promising technique to obtain novel biomaterials. **European Polymer Journal**, *in press.*

MADERUELO, C.; ZARZUELO, A.; LANAO, J. M. Critical factors in the release of drugs from sustained release hydrophilic matrices. **Journal of Controlled Release**, v. 154, p. 2–19, 2011.

MATOS, J. M. E. *et al.* Metátese de olefinas no Brasil: - "Brazil is romping it!". **Química Nova**, v. 30, p. 431–435, 2007.

MEHNERT, W.; MÄDER, K. Solid lipid nanoparticles: Production, characterization and applications. **Advanced Drug Delivery Reviews**, v. 47, p. 165–196, 2001.

MEIER, M. A. R. Metathesis with oleochemicals: New approaches for the utilization of plant oils as renewable resources in polymer science. **Macromolecular Chemistry and Physics**, v. 210, p. 1073–1079, 2009.

MEIER, M. A. R. Renewable resources for polymer chemistry: A sustainable alternative? **Macromolecular Rapid Communications**, p. 1297–1298, 2011.

MEIER, M. A. R.; METZGER, J. O.; SCHUBERT, U. S. Plant oil renewable resources as green alternatives in polymer science. **Chemical Society Reviews**, v. 36, p. 1788–1802, 2007.

MONSAERT, S. *et al.* Indenylidene-ruthenium complexes bearing saturated n-heterocyclic carbenes: Synthesis and catalytic investigation in olefin metathesis reactions. **European Journal of Inorganic Chemistry**, v. 2008, p. 432–440, 2008.

MONTERO DE ESPINOSA, L. *et al.* Fatty Acid Derived Phosphorus-Containing Polyesters via Acyclic Diene Metathesis Polymerization. **Journal of Polymer Science Part A: Polymer Chemistry**, v. 47, p. 5760–5771, 2009.

MONTERO DE ESPINOSA, L.; MEIER, M. A. R. Plant oils: The perfect renewable resource for polymer science?! **European Polymer Journal**, v. 47, p. 837–852, 2011.

MUTLU, H. *et al.* About the activity and selectivity of less well-known metathesis catalysts during ADMET polymerizations. **Beilstein Journal of Organic Chemistry**, v. 6, p. 1149–1158, 2010.

MUTLU, H. Sustainable, efficient approaches to renewable platform chemicals and polymers. 2012. 254 f. Tese (Doktors der Naturwissenschaften) – Fakultät für Chemie und Biowissenschaften, Karlsruher Institut für Technologie, Karlsruhe, 2012.

MUTLU, H.; MEIER, M. A. R. Castor oil as a renewable resource for the chemical industry. **European Journal of Lipid Science and Technology**, v. 112, p. 10–30, 2010.

MUTLU, H.; MONTERO DE ESPINOSA, L.; MEIER, M. A R. Acyclic diene metathesis: a versatile tool for the construction of defined polymer architectures. **Chemical Society Reviews**, v. 40, p. 1404–45, 2011.

NOYORI, R.; AOKI, M.; SATO, K. Green Oxidation with Aqueous Hydrogen Peroxide. **Chemical Communications,** v. 16, p. 1977-1986, 2003.

O'DONNELL, P. M. *et al.* "Perfect Comb" ADMET graft copolymers. **Macromolecules**, v. 34, p. 6845–6849, 2001.

O'BRIEN, A.K.; CRAMER, N.B.; BOWMAN, C.N. Oxygen inhibition in thiol-acrylate photopolymerizations. **Journal of Polymer Science Part A: Polymer Chemistry**, v. 44, p. 2007–2014, 2006.

ODIAN, G. **Principles of polymerization**. 4. ed. Hoboken, New Jersey: John Wiley & Sons, 2009. 839 p.

OPPER, K. L.; WAGENER, K. B. ADMET: Metathesis polycondensation. **Journal of Polymer Science Part A: Polymer Chemistry**, v. 49, p. 821–831, 2011.

PECHER, J.; MECKING, S. Nanoparticles from step-growth coordination Polymerization. **Macromolecules**, v. 40, p. 7733–7735, 2007.

PECHER, J.; MECKING, S. Nanoparticles of conjugated polymers. **Chemical Reviews**, v. 110, p. 6260–6279, 2010.

PETROVIC, Z.S. Polyurethanes from vegetable oils. **Polymer Reviews**, v. 48, p. 109–155, 2008.

PORRES, C. L. Click and Click-Type Chemistries in Castor and Sunflower Oil-Based Monomers And Polymers. 2013. 195 f. Tese (Doutorado) – Departament de Química Analítica i Química Orgànica, Universitat Rovira I Virgili, Tarragona, 2013.

POSNER, T. Beiträge zur Kenntniss der ungesättigten Verbindungen. II. Ueber die Addition von Mercaptanen an ungesättigte Kohlenwasserstoffe. **Berichte der Deutschen Chemischen Gesellschaft**, v. 38, p. 646–657, 1905.

POTAPOV, A. S. *et al.* Synthesis and oxidation of some azole-containing thioethers. **Beilstein Journal of Organic Chemistry**, v. 7, p.1526–1532, 2011.

REDDY, S. K.; ANSETH, K. S.; BOWMAN, C. N. Modeling of network degradation in mixed step-chain growth polymerizations. **Polymer**, v. 46, p. 4212–4222, 2005.

REHOR, A.; HUBBELL, J. A.; TIRELLI, N. Oxidation-Sensitive Polymeric Nanoparticles. **Langmuir,** v. 21 (1), 411−417, 2005.

REHOR, A.; TIRELLI, N.; HUBBELL, J. A. A New Living Emulsion Polymerization Mechanism: Episulfide Anionic Polymerization. **Macromolecules**, v. 35, p. 8688−8693, 2002.

ROMIO, A. P. *et al.* Encapsulation of magnetic nickel nanoparticles via inverse miniemulsion polymerization. **Journal of Applied Polymer Science**, v. 129, p. 1426–1433, 2013.

RONDA, J. C. *et al.* Vegetable oils as platform chemicals for polymer synthesis. **European Journal of Lipid Science and Technology**, v. 113, p. 46–58, 2011.

RYBAK, A.; FOKOU, P. A.; MEIER, M. A. R. Metathesis as a versatile tool in oleochemistry. **European Journal of Lipid Science and Technology**, v. 110, p. 797–804, 2008.

RYBAK, A.; MEIER, M. A R. Acyclic diene metathesis with a monomer from renewable resources: control of molecular weight and one-step preparation of block copolymers. **ChemSusChem**, v. 1, p. 542–547, 2008.

RYDHOLM, A. E.; ANSETH, K. S.; BOWMAN, C. N. Effects of neighboring sulfides and pH on ester hydrolysis in thiol-acrylate photopolymers. **Acta Biomaterialia**, v. 3, p. 449–455, 2007.

RYDHOLM, A. E.; BOWMAN, C. N.; ANSETH, K. S. Degradable thiol-acrylate photopolymers: Polymerization and degradation behavior of an in situ forming biomaterial. **Biomaterials**, v. 26, p. 4495– 4506, 2005.

SCHORK, F. J. *et al.* Miniemulsion polymerization. **Advances in Polymer Science**, v. 175, p. 129–255, 2005.

SCHROCK, R. *et al.* Preparation and characterization of active niobium, tantalum and tungsten metathesis catalysts. **Journal of Molecular Catalysis**, v. 8, p. 73–83, 1980.

SHARMA, V.; KUNDU, P. P. Addition polymers from natural oils — A review. **Progress in Polymer Science**, v. 31, p. 983–1008, 2006.

SHARMA, V.; KUNDU, P. P. Condensation polymers from natural oils. **Progress in Polymer Science**, v. 33, p. 1199–1215, 2008.

STAUDT, T. *et al.* Magnetic polymer/nickel hybrid nanoparticles via miniemulsion polymerization. **Macromolecular Chemistry and Physics**, v. 214, p. 2213–2222, 2013.

STENZEL, M. H. Bioconjugation using thiols : Old chemistry rediscovered to connect. **ACS Macro Letters**, v. 2, p. 14–18, 2013.

TAKAGAKI, A. *et al.* Esterification of higher fatty acids by a novel strong solid acid. **Catalysis Today**, v. 116, p. 157–161, 2006.

TIARKS, F.; LANDFESTER, K.; ANTONIETTI, M. Preparation of polymeric nanocapsules by miniemulsion polymerization. **Langmuir**, v. 17, p. 908–918, 2001.

TÜRÜNÇ, O. Efficient Routes to Degradable and non-Degradable Renewable Polymers from Fatty Acids. 2012. 211 f. Tese (Doktors der Naturwissenschaften) – Fakultät für Chemie und Biowissenschaften, Karlsruher Institut für Technologie, Karlsruhe, 2012.

TÜRÜNÇ, O.; MEIER, M. A. R. A novel polymerization approach via thiol-yne addition. **Journal of Polymer Science Part A: Polymer Chemistry**, v. 50, p. 1689–1695, 2012.

TÜRÜNÇ, O.; MEIER, M. A. R. Fatty acid derived monomers and related polymers via thiol-ene (click) additions. **Macromolecular Rapid Communications**, v. 31, p. 1822–1826, 2010.

TÜRÜNÇ, O.; MEIER, M. A. R. The thiol-ene (click) reaction for the synthesis of plant oil derived polymers, **European Journal of Lipid Science Technology**, v. 115, p. 41–54, 2013.

TÜRÜNÇ, O.; MEIER, M. A. R. Thiol-ene vs. ADMET: a complementary approach to fatty acid-based biodegradable polymers. **Green Chemistry**, v. 13, p. 314, 2011.

UGELSTAD, J.; EL-AASSER, M. S.; VANDERHOFF, J. W. J. Emulsion polymerization: Initiation of polymerization in monomer droplets. **Journal of Polymer Science: Polymer Letters Edition**, v. 11, p. 503–513, 1973.

VAN DEN BERG, O. *et al*. Renewable sulfur-containing thermoplastics via AB-type thiol-ene polyaddition. **European Polymer Journal,** v. 49, p. 804–812, 2013.

VAN DER STEEN, M.; STEVENS, C. V. Undecylenic acid: A valuable and physiologically active renewable building block from castor oil. **ChemSusChem**, v. 2, p. 692–713, 2009.

VANDENBERGH, J. *et al.* Cross-linked degradable poly(β-thioester) networks via amine-catalyzed thiol-ene click polymerization. **Polymer**, v. 55, p. 3525–3532, 2014.

VO, C. D.; KILCHER, G.; TIRELLI, N. Polymers and Sulfur: what are Organic Polysulfides Good For? Preparative Strategies and Biological Applications. **Macromolecular Rapid Communications**, v. 30, p. 299−315, 2009.

WAGENER, K. B. *et al*. The key to successful acyclic diene metathesis polymerization chemistry. **Makromolekulare Chemie**, v. 191, p. 365–374, 1990b.

WAGENER, K.B. *et al*. Acyclic Diene Metathesis Copolymerization of 1,5-Hexadiene and 1,9-Decadiene. **Macromolecules**, v. 23, p.5155–5157, 1990a.

WANG, J. J. *et al*. Lipid nanoparticles with different oil/fatty ester ratios as carriers of buprenorphine and its prodrugs for injection. **European Journal of Pharmaceutical Sciences**, v. 38, p. 138–146, 2009.

WANG, K. *et al*. Preparation and properties of cyclic acetal based biodegradable gel by thiol-ene photopolymerization. **Materials Science and Engineering: C**, v. 33, p. 1261–1266, 2013.

WARWEL, S. *et al.* Polymers and surfactants on the basis of renewable resources. **Chemosphere**, v. 43, p. 39–48, 2001.

WURM, F. R.; WEISS, C. K. Nanoparticles from renewable polymers. **Frontiers in Chemistry**, v. 2 , 49, 2014.

YU, T. *et al*. The double melting peaks of poly(ethylene terephthalate). **Polymer Communications**, p. 83–91, 1983.

YU, T.; MALUGIN, A.; GHANDEHARI, H. Impact of silica nanoparticle design on cellular toxicity and hemolytic activity. **ACS Nano**, v. 5, p. 5717–5728, 2011.

ZOU, J. *et al.* Clicking well-defined biodegradable nanoparticles and nanocapsules by UV-induced thiol-ene cross-linking in transparent miniemulsions. **Advanced Materials**, v. 23, p. 4274–4277, 2011.

ATTACHMENTS

A1. EXTRA REACTIONS

Thiol-ene reactions in miniemulsion, using 1,7-octadiene and 1,4-butanedithiol as comonomers,1 mol% AIBN and Crodamol™ GTCC (MiniE1) or Hexadecane (MiniE2) as costabilizers. Bulk reaction (Bulk E) at the same conditions (but without costabilizer) for comparison. Stable lattices were obtained when using both costabilizers and similar molecular weight results were achieved when compared to the bulk reaction.

Entry	Costabilizer	Dp (nm)	M_n (kDa) [a]	M_w (kDa) [a]
Bulk E	-	-	3.4	9.1
MiniE1	Crodamol®	145	5.1	14.2
MiniE2	Hexadecane	153	6.8	14.9